

## Fermilab Test Beam Facility Annual Report: FY18

M. Rominsky<sup>1</sup> E. Schmidt<sup>1</sup> S. Amaral<sup>2</sup> G. Auzinger<sup>2</sup>  
 R. Ceccarelli<sup>3</sup> X. Chen<sup>4</sup> T. Cheng<sup>5</sup> G. Chiodini<sup>6</sup> R. Coluccia<sup>6</sup>  
 M. Delcourt<sup>5</sup> M. Dinardo<sup>7</sup> A. Fiaschi<sup>3</sup> F. Golf<sup>8</sup> G. Hanson<sup>9</sup>  
 M. Haranko<sup>10</sup> F. Jensen<sup>11</sup> M. Jones<sup>5</sup> A. Khatiwada<sup>5</sup> M. Krohn<sup>11</sup>  
 C. Mantilla<sup>12</sup> M. Mieschini<sup>3</sup> L. Moroni<sup>7</sup> A. Nazario<sup>13</sup>  
 S. Norberg<sup>13</sup> W. Ortiz<sup>13</sup> R. Rivera<sup>1</sup> B. Schneider<sup>1</sup>  
 S. Seif-El Nasr Storey<sup>14</sup> W. Si<sup>15</sup> L. Uplegger<sup>1</sup> C. Vernieri<sup>1,24</sup>  
 L. Viliani<sup>3</sup> S. Wagner<sup>11</sup> G. Zevi Della Porta<sup>16</sup> D. Zuolo<sup>7</sup>  
 B. Bylsma<sup>17</sup> B. Cardwell<sup>17</sup> S. Dittmer<sup>4</sup> A. Frankenthal<sup>15</sup> C. Hill<sup>17</sup>  
 C. Mills<sup>4</sup> C. Adams<sup>18</sup> J. Asaadi<sup>19</sup> M. Auger<sup>20</sup> W. Badgett<sup>1</sup>  
 D. Barker<sup>21</sup> V. Basque<sup>22</sup> R. Carey<sup>23</sup> A. Ereditato<sup>20</sup> A. Falcone<sup>19</sup>  
 R. C. Fernandez<sup>1</sup> D. Goeldi<sup>20</sup> R. Guenette<sup>24</sup> F. Kamiya<sup>25</sup>  
 E. Kemp<sup>26</sup> I. Kreslo<sup>20</sup> R. Lazur<sup>27</sup> D. Lorca<sup>20</sup> A. A. B Machado<sup>25</sup>  
 L. M. Santos<sup>26</sup> M. Mooney<sup>27</sup> C. A. Moura<sup>25</sup> P. D. Neto<sup>26</sup>  
 M. Nunes<sup>26</sup> L. Paulucci<sup>25</sup> G. Pulliam<sup>28</sup> D. Sessumes<sup>19</sup>  
 J. Sinclair<sup>20</sup> M. Soderberg<sup>28</sup> N. Sponer<sup>21</sup> J. St. John<sup>1</sup>  
 H. Sullivan<sup>19</sup> A. Szelc<sup>22</sup> K. Terao<sup>29</sup> I. C. Terrazas<sup>27</sup> A. Tripathi<sup>19</sup>  
 Y. Tsai<sup>29</sup> M. Weber<sup>20</sup> Z. Williams<sup>19</sup> J. Freeman<sup>1</sup> D. Lincoln<sup>1</sup>  
 R. Belmont<sup>11</sup> S. Boose<sup>30</sup> E. Desmond<sup>30</sup> J. Frantz<sup>31</sup> J. Haggerty<sup>30</sup>  
 J. Huang<sup>30</sup> E. Gamez<sup>32</sup> N. Grau<sup>33</sup> D. Isreal<sup>33</sup> Y. Kim<sup>34</sup>  
 E. Kistenev<sup>30</sup> J. Lajoie<sup>36</sup> S. Lee<sup>33</sup> N. Lewis<sup>32</sup> E. Mannel<sup>30</sup>  
 J. Mazer<sup>32</sup> J. Osborn<sup>37</sup> M. Patel<sup>36</sup> R. Pisani<sup>30</sup> C. Pontieri<sup>30</sup>  
 D. Perepelitsa<sup>11</sup> A. Pun<sup>31</sup> M. Purschke<sup>30</sup> A. Romero Hernandez<sup>33</sup>  
 J. Runchey<sup>33</sup> Z. Shi<sup>38</sup> S. Stoll<sup>30</sup> F. Toldo<sup>30</sup> C. Woody<sup>30</sup>  
 Koji Nakamura<sup>39</sup> Shun Ono<sup>39</sup> Miho Yamada<sup>39</sup> Toru Tsuboyama<sup>39</sup>  
 Kazuhiko Hara<sup>40</sup> Manabu Togawa<sup>39</sup> Minoru Hirose<sup>41</sup> J. Metcalfe<sup>35</sup>  
 M. Benoit<sup>42</sup> M. Barreto Pinto Vicent<sup>42</sup> V. Bhopatkar<sup>35</sup> W. Islam<sup>43</sup>  
 M. Kiehn<sup>42</sup> J. Lambert<sup>44</sup> J. Muse<sup>44</sup> J. Xie<sup>35</sup>  
 J. Paley<sup>1</sup> for the EMPHATIC Collaboration A. Apresyan<sup>1</sup> S. Xie<sup>45</sup>  
 S. Aune<sup>46</sup> B. Azmoun<sup>30</sup> I. Mandjavidze<sup>46</sup> H. Pereira-Da-Costa<sup>46</sup>  
 M. Vandenbroucke<sup>46</sup> R. Nouicer<sup>30</sup> Y. Akiba<sup>47,48</sup> E. Desmond<sup>30</sup>  
 M. Hidekazu<sup>47,48</sup> G. Mitsuka<sup>48</sup> I. Nakagawa<sup>47,48</sup> T. Hachiya<sup>48,50</sup>  
 Y. Yamaguchi<sup>52</sup> X. He<sup>52</sup> W. Rho<sup>52</sup> X. Sun<sup>52</sup> S. Syed<sup>52</sup>  
 M. Contalbrigo<sup>53</sup> L. Barion<sup>53</sup> V. Lucherini<sup>53</sup> T. Lam<sup>54</sup>

I. Mostafanezhad<sup>54</sup>    G. Varner<sup>54</sup>    M. Chiu<sup>30</sup>    F. Cao<sup>35</sup>  
 M. Hattawy<sup>35</sup>    E. May<sup>35</sup>    J. Xie<sup>35</sup>    W. Xi<sup>55</sup>    H. van Hecke<sup>51</sup>  
 S. Lim<sup>51</sup>    M. Liu<sup>51</sup>    D. McGlinchey<sup>51</sup>    A. Tkatchev<sup>51</sup>    S. Uemura<sup>51</sup>  
 K. Dehmelt<sup>56</sup>, P. Garg<sup>56</sup>, K. Gnanvo<sup>57</sup>, M. Hohlmann<sup>58</sup>, T. K. Hemmick<sup>56</sup>  
 V. Canoe-Roman<sup>56</sup>    N. Ram<sup>56</sup>    L. Legnosky<sup>56</sup>    S. Slote<sup>56</sup>    I. Yousuf<sup>56</sup>  
                                  V. Zakharov<sup>56</sup>

<sup>1</sup>Fermi National Accelerator Laboratory

<sup>2</sup>European Organisation for Nuclear Research (CERN)

<sup>3</sup>INFN Florence

<sup>4</sup>University of Illinois at Chicago

<sup>5</sup>Purdue University

<sup>6</sup>INFN Lecce

<sup>7</sup>INFN Milan

<sup>8</sup>University of Nebraska

<sup>9</sup>University of California, Riverside

<sup>10</sup>DESY

<sup>11</sup>University of Colorado at Boulder

<sup>12</sup>John Hopkins University

<sup>13</sup> Puerto Rico University

<sup>14</sup> University of Bristol

<sup>15</sup> Cornell

<sup>16</sup> University of California, San Diego

<sup>17</sup>The Ohio State University

<sup>18</sup> Harvard

<sup>19</sup>University of Texas at Arlington

<sup>20</sup> Universitaet Bern

<sup>21</sup> University of Sheffield

<sup>22</sup> University of Manchester

<sup>23</sup> Boston University

<sup>24</sup> Oxford

<sup>25</sup> UFABC

<sup>26</sup> UNICAMP

<sup>27</sup> Colorado State University

<sup>28</sup> Syracuse University

<sup>29</sup> SLAC

<sup>30</sup>Brookhaven National Laboratory

<sup>31</sup> Ohio State University, Athens OH

<sup>32</sup>Rutgers University

<sup>33</sup> Augustana University

- <sup>34</sup> University of Illinois Urbana Champaign  
<sup>35</sup> Argonne National Laboratory  
<sup>36</sup> Iowa State University  
<sup>37</sup> University of Michigan  
<sup>38</sup> Massachusetts Institute of Technology  
<sup>39</sup> High Energy Accelerator Research Organization (KEK)  
<sup>40</sup> University of Tsukuba  
<sup>41</sup> Osaka University  
<sup>42</sup> Université de Genève  
<sup>43</sup> Oklahoma State University  
<sup>44</sup> University of Oklahoma  
<sup>45</sup> Caltech  
<sup>46</sup> CEA Saclay  
<sup>47</sup> Nishina Center for Accelerator Based Science, RIKEN  
<sup>48</sup> RIKEN-BNL Research Center  
<sup>49</sup> Department of Physics, Rikkyo University  
<sup>50</sup> Department of Physics, Nara Women's University  
<sup>51</sup> Los Alamos National Laboratory  
<sup>52</sup> Georgia State University  
<sup>53</sup> INFN Ferrara  
<sup>54</sup> University of Hawaii  
<sup>55</sup> Thomas Jefferson National Accelerator Facility  
<sup>56</sup> Stony Brook University  
<sup>57</sup> University of Virginia  
<sup>58</sup> Florida Institute of Technology

February 12, 2019

### **Abstract**

This Technical Memorandum (TM) summarizes the Fermilab Test Beam operations for FY2018. It is one of a series of annual publications intended to gather information in one place. This TM discusses the experiments performed at the Test beam from November 2017 to July 2018. The experiments are listed in Table 1. Each experiment wrote a summary that was edited for clarity and is included in this report.

## **1 Summary of FY18**

The Fermilab Test Beam Facility continues to be an important resource for experiments and for detector R&D. In FY18, we supported a very heavy load of users, primarily from

the collider physics community. Beam was nearly completely dominated by user requests, with only a few days dedicated to facility studies and improvements. Highlights from the FY18 year include:

- Hosting the Excellence in Detectors School (EDIT) at Fermilab, which the test beam was an integral part of.
- Hosting summer interns. This year, they worked to improve the slow control system for the Cherenkov, wrote data acquisition code, and improved virtual machine tools.
- Both MCenter and MTest were utilized during the full year. In MCenter, users both used the beam and preparations started for the NOvA test beam.
- *otsdaq* code has been written for all the facility instruments and we hope to commission a DAQ this year.
- We hired an Applications Physicist to help with projects and coordination.

During the FY18 year, we hosted twenty experiments (Table 1) and the Excellence in Detectors and Technology (EDIT) School. The EDIT school consisted of 48 students who were selected by an international committee to spend two weeks at Fermilab learning about detectors. The test beam track had students working in both MCenter and MTest. In MCenter, they learned to set up an experiment - cabling, setting up a simple data acquisition system, and setting up instruments. In MTest, they took data using the facility instruments. They were split into two teams and one group used the wire chambers to take data while a second used the Cherenkov. They practiced taking data, making plots, and working as a team to mount a test beam run. During the EDIT school, we continued to have users take beam during the overnight hours in the MTest beamline.

Throughout the year, we worked on the data acquisition system for the test beam and had some success. The *otsdaq* platform now has all the instrumentation in it, but still needs some tweaking to make sure it all works together. We are currently in the process of testing the separate frontends and then forming them into a coherent configuration.

This year was particularly busy at the test beam. Out of the thirty five weeks of running, thirty four weeks had more than one user in them, and fifteen weeks had more than two experiments running. During one particularly time period, we had five experiments running in parallel. These groups were typically from the same experiment and worked well together.

The Accelerator delivered over 170,00 pulses to the test beam, as seen in Figure 1. We are grateful to the accelerator for the beam they delivered to us.

## 2 Research Overview at the Test Beam

In FY18, we had a large group of users from the collider physics, with many testing irradiated sensors. The individual reports in the next section fully describe the tests that



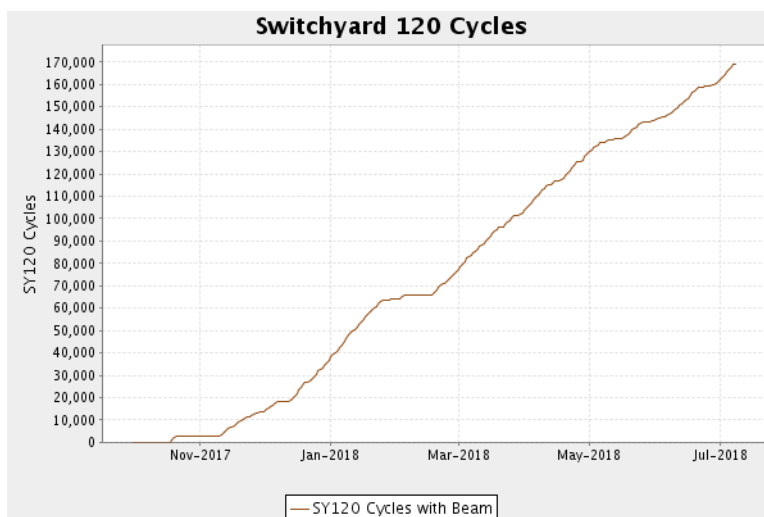


Figure 1: Delivery of pulses to the test beam. Note that this includes data sent to both MCenter and MTest. The flat regions represent change overs or problems in the beam. Note the long flat region in February. This represents time lost due to a magnet change out.

were carried out.

## 2.1 Publications

The groups at the test beam will often report their findings in internal notes, at conferences, and in published journals. This past year, all twenty groups have plans for publications or have presented results at conferences. This year, there were 5 articles published in journals, with several in preparation.

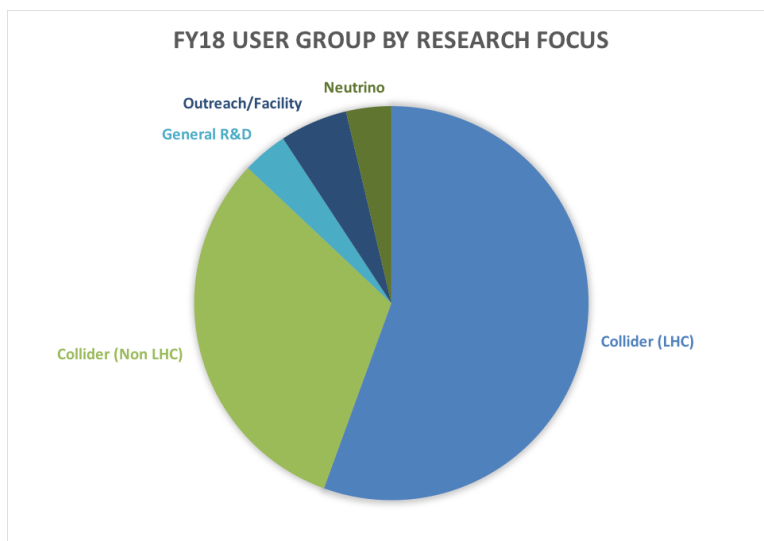


Figure 2: Breakdown of FY18 users by research focus. This year, we had a large group of collider experiments.

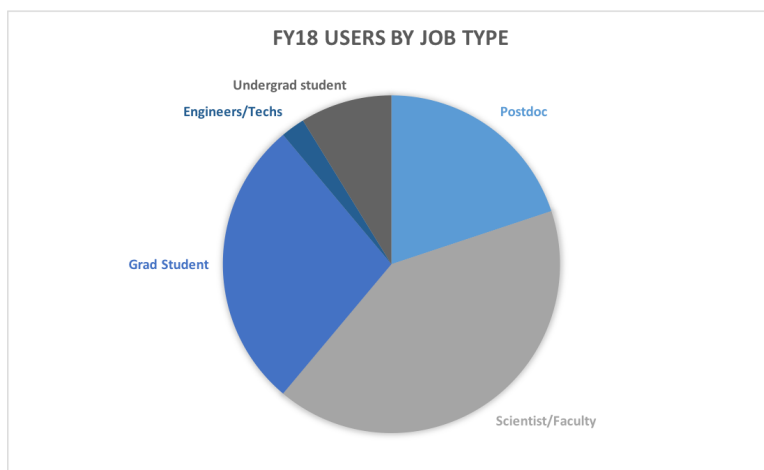


Figure 3: Breakdown of FY18 users by professional class.

Experiment Number	Description
T0992	INFN CMS Pixels Phase II Sensors
T0992	US CMS Pixels Phase II Sensors
T0992	RD53a Chip Tests
T0992	CMS Outer Tracker Phase 2
T0992	Fermilab FCP130
T1034	LArIAT: Liquid Argon in a Test Beam
T1041	CMS Forward Calorimetry R&D
T1044	sPHENIX Calorimetry Tests
T1068	Beam Tests of the SVX4 Telescope
T1209	CMS Outer Tracker R&D (MAPSA)
T1224	ATLAS Pixel Telescope Tests
T1297-02	PixLAr
T1396	EMPHATIC (Hadron Emulsion Detectors for Neutrinos)
T1409	CMS Timing Tests
T1429	Performance Study of a planar GEM and MM detector with zigzag pad readout
T1439	sPHENIX Silicon Strip Tracker (INTT) Testsu
T1441	sPHENIX MAPS Vertex Detector (MVTX)
T1443	SBND Vertical Slice Test
T1450	EIC PID R&D: Argonne MCP-PMT Test
T1473	FLYSUB-Consortium Tracking and RICH Performance Evaluation
EDIT	Excellence in Detector and Instrumentation Techniques School

Table 1: Test Beam experiments performed in FY18.

FTBF FY18 By the Numbers	
<i>Professional Class</i>	<i>Total</i>
Postdoc	43
Scientist/Faculty	89
Graduate Student	60
Engineers/Techs	5
Undergraduate students	19
Total	215
<i>Experiment Focus (TSWs)</i>	<i>Total</i>
Neutrino	2
Collider (LHC)	30
Collider (Non-LHC)	17
General R&D	2
Outreach/Facility	3
<i>Publications</i>	<i>total</i>
Journals	4
Conference proceedings/presentations	3
Posters	4 and counting
Internal Notes	Information coming

Table 2: Statistics for Test Beam experiments performed in FY18. Note that the Experiment focus is listed in weeks of beam taken by the group.

### 3 T992: Tests of Radiation-hard Sensors for the HL-LHC

*R. Rivera, L. Uplegger, et. al*

**Beam used:** 120 GeV protons.

**Run dates:** Nov 1 - Dec 12, 2017. Jan 31 - Feb 20, May 2 - June 5, 2018

#### Motivation and Goals

At the HL-LHC, after  $2500 \text{ pb}^{-1}$  of data, the Expected maximum fluence for the pixel region ( $< 20 \text{ cm}$ ) will be  $2.5 \times 10^{16}$  neutron-equivalent per  $\text{cm}^2$ . To cope with this unprecedented radiation environment, there have been quite a few international collaborations formed to find possible solutions for vertex and tracking detectors at the HL-LHC. These include the RD42, RD49, and RD50 collaborations. A variety of solutions have been pursued. These include diamond sensors, 3D sensors, MCZ planar silicon detectors made from MCZ wafers, epitaxial, p-type silicon wafers and thin silicon detectors. The experimenters wish to compare the performance of this wide variety of detectors in a test beam before and after irradiation. To do so, the experimenters use the FTBF pixel and strip tracking telescopes which have  $\approx 8 \mu\text{m}$  resolution at the device under test. In particular, the experimenters are planning to study the charge collection efficiency of irradiated and un-irradiated devices and the spatial resolution as a function of the applied sensor voltage bias and the track incident angle. For the foreseen upgrade in luminosity CMS will also upgrade the strip tracker and the new Read Out Chip (ROC) need to be tested in more realistic conditions than on a test bench. Pixel-Strip and Strip-Strip sensors configuration has been tested to study detector efficiency and time walk.

#### Setup

The pixel and strip telescopes are read out through a custom DAQ system known as CAPTAN. A gigabit Ethernet board is used to route UDP data to a computer which is connected to a Fermilab server via internet. The readout boards are located close to the detector in the hut, and share a common clock and trigger signal. The detectors themselves may be operated up to  $\approx 800 \text{ V}$ .

#### Results and Publications

The experimenters studied 3D silicon, a new prototype of planar sensors with a small pitch ( $25 \mu\text{m}$ ) and several n-on-p type silicon thin planar sensors. 3D tracking detectors and thin n-on-p sensors are promising radiation-hard candidates to replace planar n-on-n detectors

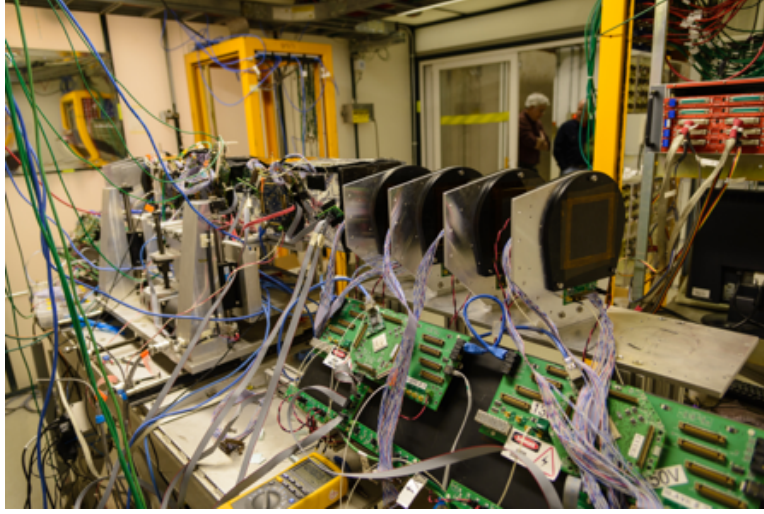


Figure 4: CMS Pixel telescope located in the MTest beamline, section 6.1a

in the HL-LHC. Radiation damage effects are measured with regards to charge collection, efficiency, and resolution of the particle tracks in beam tests, as well as leakage current and pixel noise. We have studied two varieties of 3D sensors: 1E, 2E (the number referring to the number of implant pattern per pixel), irradiated at CERN and in a neutron reactor in Ljubljana with doses up to  $1 \times 10^{16}$  neq/cm<sup>2</sup>. The 3D devices are fabricated at the Fondazione Bruno Kessler (FBK) in Italy, while thin n-on-p sensors are fabricated at FBK and HPK. These new devices have all patterns with pitches of 25 or 50  $\mu$  m. Different designs, mostly with different bias schemes, were tested to compare their performance before and after irradiation to converge to the most efficient and radiation hard fabrication process. These combined efforts from the European, testing devices from FBK, and US collaborators, testing devices from FBK, is narrowing down the possible candidates for the upgrade and is also converging on the final design that will then be mounted on the new read out chip coming from the RD53 collaboration.

The collaboration is also testing devices for the CMS Outer Tracker phase II upgrade and in December 2017 and May 2018 a new prototype of strip-strip (2S) module was tested. The module was the first prototype with the new and almost final design of the read out chip called CBC3. In December we measured efficiency, charge collection, time walk and assess the overall properties of the chip which worked as expected. In May instead, after being irradiated to  $2 \times 10^{14}$  neq/cm<sup>-2</sup>, the module was re-tested to check the overall performances to a dose that is close to the maximum expected in HL-LHC. The module performed very well before and after irradiation increasing the confidence in the collaboration to have already a reliable and working candidate for the upgrade.

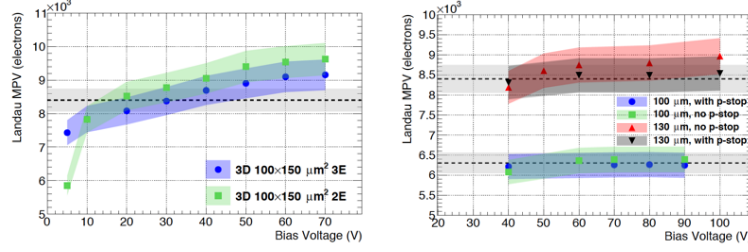


Figure 5: (Left) Landau Most Probable Value (MPV) as a function of the bias voltage for non-irradiated thin planar sensors. (Right) Landau Most Probable Value (MPV) as a function of the bias voltage for non-irradiated 3D sensors.

## 4 T992: RD53a Chip Tests

*B. Bylsma, B. Cardwell, S. Dittmer, A. Sterenberg Frankenthal, C. Hill, C. Mills*

**Beam used:** 120 GeV protons.

**Run dates:** May 2 - June 5, 2018

## Motivation and Goals

The CMS pixel detector upgrade for the HL-LHC must withstand unprecedented radiation fluence, up to  $2 \times 10^{16}$  neutron-equivalent per  $\text{cm}^2$  over the lifetime of the detector. To deliver the precision tracking needed to discriminate the 200 interactions per bunch crossing while withstanding the radiation dose, improvements to both the sensors and readout chips (ROCs) are needed. The first prototype of the ROC, the RD53A chip, has been available for testing starting in April-May 2018.

Our primary goal for this past summer was to integrate the RD53A readout with the beam telescope at FBTF. This sets the foundations for future work at the Fermilab testbeam in the coming fall and winter.

The test-beam program at FNAL in the next year will test the radiation hardness of the proposed pixel sensors and ROCs. Using facilities at Los Alamos National Laboratory, US-CMS will irradiate ROC+sensor assemblies to the full radiation dose expected for the innermost layers of the pixel detector during the HL-LHC. These assemblies will be tested at the Fermilab test beam before (November) and after (February) that irradiation, using the infrastructure we commissioned last summer. Our team will have the unique ability to test the performance of the sensors and ROCs after the full expected radiation dose.

## Setup

Our RD53a assembly was set up in Area 6.1a of FBTF with the silicon-strip telescope, as shown in Fig. 6. The DUT was read out using the Yarr software from a standalone PC placed in the enclosure. The PC had an FPGA board (an XPressK7) mounted in the PCIe slot on the motherboard, with daughter cards designed by the OSU team to connect to the DUT and bring in the external trigger signal from the scintillator in the telescope. The sensor was biased to 80V.

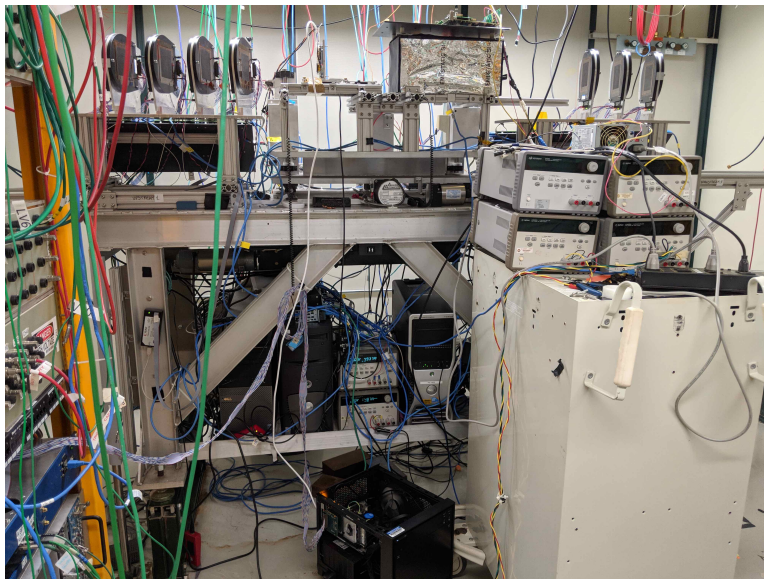


Figure 6: Configuration of the RD53A sensor+ROC assembly (top center) in the beamline showing the strip telescope and the PC used for readout.

## Results and Publications

Our group tested an RD53A sensor+ROC assembly to commission the functionality of reading out this completely new chip with new DAQ (Yarr) and the silicon-strip telescope. Working with Timon Heim at LBNL, the primary developer of the Yarr DAQ software, our team integrated the Yarr readout software with the OTSDAQ readout used for the telescope so that their readout could be synchronized. The OSU team produced hardware and Timon wrote firmware to bring in an external trigger, with technical assistance from Lorenzo Uplegger. This was perhaps most challenging part of the operation. After that, the relative timing of the trigger-accept window for the DUT could be aligned with the signals from the telescope to produce events which contained both hits from the DUT and



tracks from the telescope. Our team also wrote software, with Lorenzo, to merge these data streams for analysis of hit resolutions, efficiencies, and related quantities.

After synchronizing the DUT with the telescope trigger, we recorded the detector occupancy for the two operating front-ends. The occupancy heat map, shown in Fig. ??, clearly shows the beamspot. The RD53A contains three different analog front-end designs, which can clearly be seen here. In the interest of time, one front end was masked off and the other two are not optimized so they have different efficiencies. Analysis of the results is ongoing, in part to prepare for the upcoming test beams with more ROCs and sensor types.

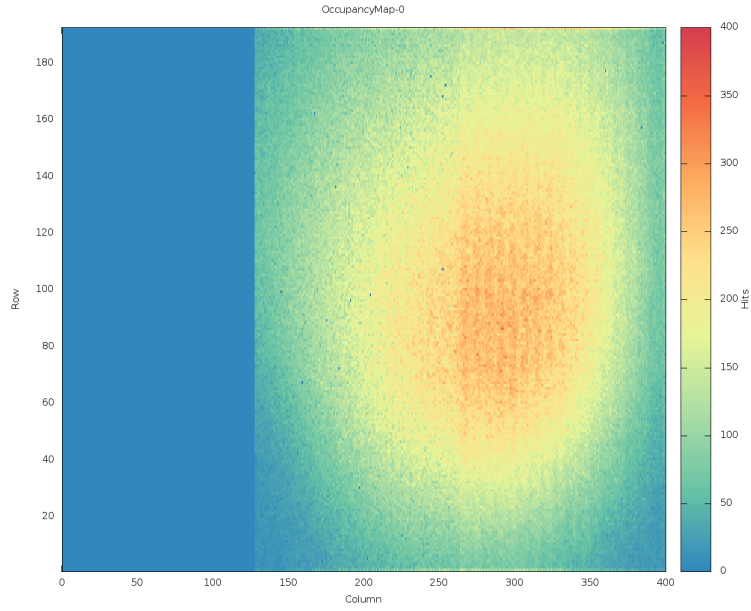


Figure 7: Occupancy plot showing beamspot in the RD53A DUT.

## 5 T1034: LArIAT and PixLar

*J. Asaadi, M. Auger, W. Badgett, D. Barker, V. Basque, R. Carey, A. Ereditato, A. Falcone, R. C. Fernandez, D. Goeldi, R. Guenette, F. Kamiya, E. Kemp, I. Kreslo, R. Lazur, D. Lorca, A. A. B Machado, L. M. Santos, M. Mooney, C. A. Moura, P. D. Neto, M. Nunes, L. Paulucci, G. Pulliam, D. Sessumes, J. Sinclair, M. Soderberg, N. Sponer, J. St. John, H. Sullivan, A. Szelc, K. Terao, I. C. Terrazas, A. Tripathi, Y. Tsai, M. Weber, Z. Williams*

**Beam used:** 8-64 GeV  $pi^{+/-}$

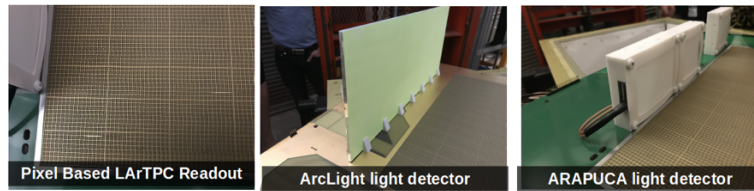
**Run dates:** December 2017 - January 2018

### Motivation and Goals

LArIAT (Liquid Argon in a Test beam) is an experiment set to calibrate the liquid Argon Time Projection Chamber technology (LArTPC) by placing the detector in a beam of charged particles of known type and momentum. In the configuration used during the PixLar run the wire planes were replaced with a pixel based readout to access the feasibility of utilizing and reconstructing data from a pixel based LArTPC in a high multiplicity environment. Additionally, new light readout techniques were deployed including the ArcLight device from University of Bern and a new version of the ARAPUCA light trap from UNICAMP and UFABC.

### Setup

The LArIAT TPC was repurposed with a pixel based anode plane of 28,800 pixels in two 36 cm x 36 cm active area. Along the upstream and downstream areas of the TPC the ArcLight and ARAPUCA devices were deployed. In order to readout all 28,800 pixels using the existing 480 cold electronics channel, the pixel readout was multiplexed with the disambiguation to be done offline using matching between regions of interest and the corresponding pixel.



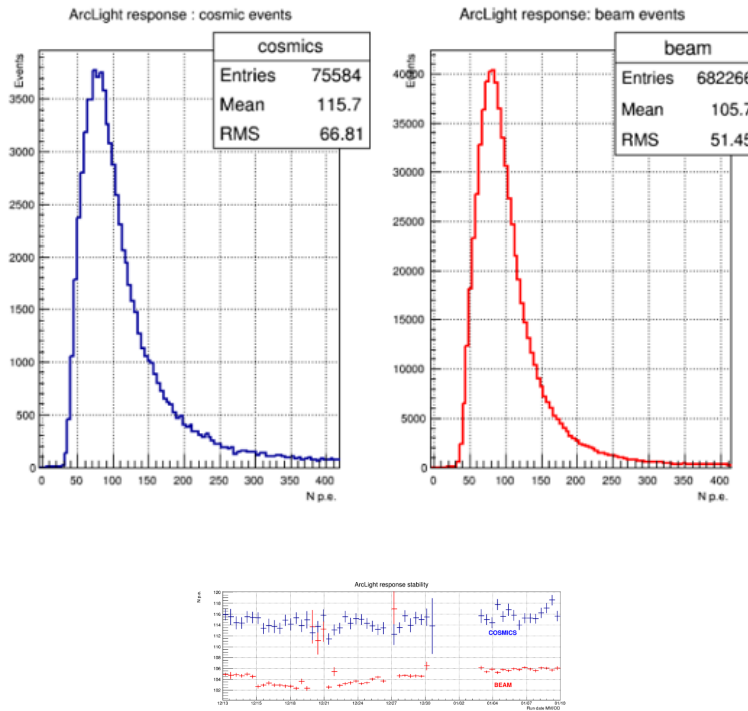
The remainder of the beamline setup was left unchanged from the previous LArIAT

runs providing both cosmic triggers in addition to the ability to identify the incoming charged particle species type and momentum from the beamline.

## Results and Publications

**Light Detection Results:** ArcLight showed stable and similar response to both cosmics and beam. Ongoing work to associate individual light signatures to individual tracks continues for absolute calibration of the device.

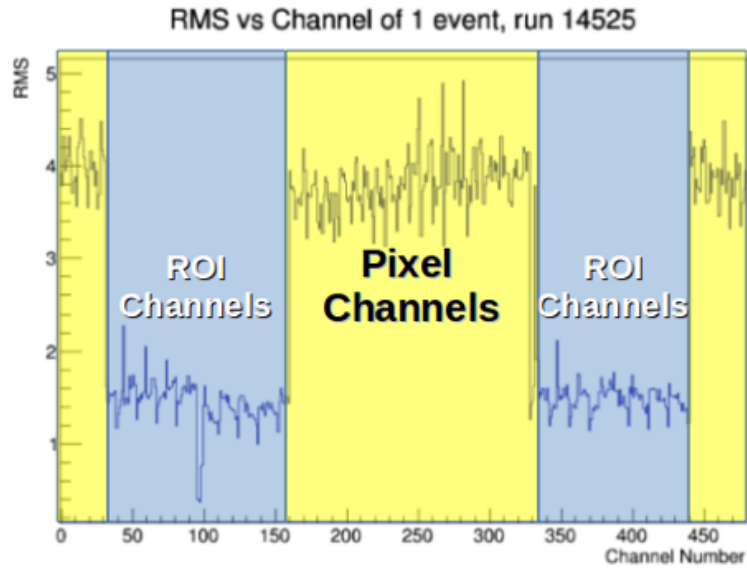
The ArcLight is now considered as the preferred light detection device for the liquid argon near detector for DUNE based on its performance in the PixLAr setup.



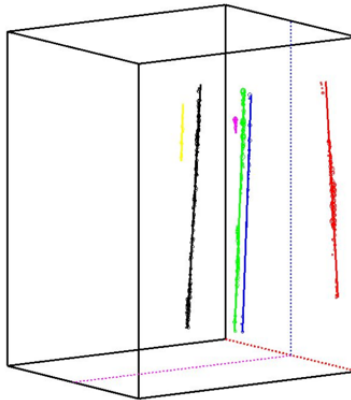
**Charge Detection Results:** 13:1 signal to noise on the multiplexed pixel channels demonstrates the clear viability of the dedicated pixel based readout. Moreover, dedicated pixel based readout electronics (LArPix) will forgo the need for the multiplexing used in this iteration of PixLAr, thus further enhancing the physics potential this type of readout.

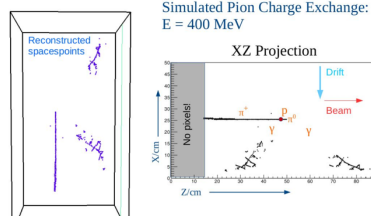
High multiplicity events (>6 tracks) can unambiguously be reconstructed in the TPC along with complex topologies such as pion charge exchange ( $p^+ \rightarrow p^0 \rightarrow gg$ ) being observed in data and simulation. Ongoing reconstruction work aims to demonstrate the pure 3d reconstruction techniques, perform the electron lifetime measurement, and demonstrate the high multiplicity capabilities of the pixel based LArTPC.

Publication of the detector paper performance as well as a technical publication on the reconstruction techniques is expected in the coming months.



### Clustering and Tracking





## 6 T1041: CMS Forward Calorimetry R&D

*J. Freeman, D. Lincoln*

**Beam:** 120 GeV protons

**Run dates:** January 2018 to July 2018 (parasitic)

### Motivation and Goals

CMS is developing an upgraded calorimeter for the HL-LHC. We are studying SiPM-on-tile designs to be used in the Back Hadron forward calorimeter. We have built a triggered DRS4 system with computer-controlled x-y positioning. We raster the test objects through the testbeam and measure light yield for each trigger point (3x3mm).

### Setup

The test setup, shown in Figure 8, was a remote controlled x-y stage with a small dark box attached. Inside the dark box was the sample SiPM-on-Tile. The SiPM was read out by a DRS4 waveform digitizer.

### Results and Publications

Numerous tests have been performed here. Important results include: verification of the extremely high reflectivity of the ESR foil; determination of uniformity of SiPM-on-tile designs; measurement of LY vs tile size; measurement of LY vs tile thickness; cross calibration of radioactive source scan results from NIU; demonstration that radiation damage in scintillator is due to local primary scintillation light loss and not to bulk attenuation (of the CMS calorimeter geometries).

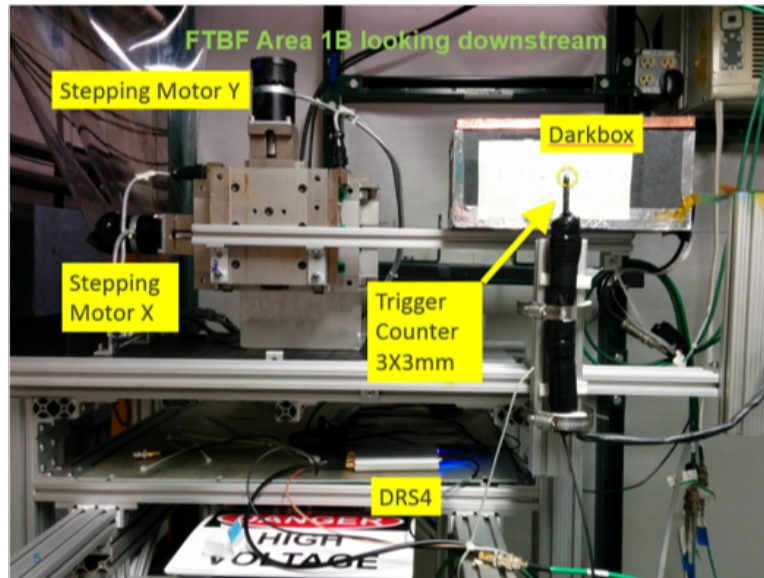


Figure 8: Setup for the T1041 experiment in MTest, section 6.1b.

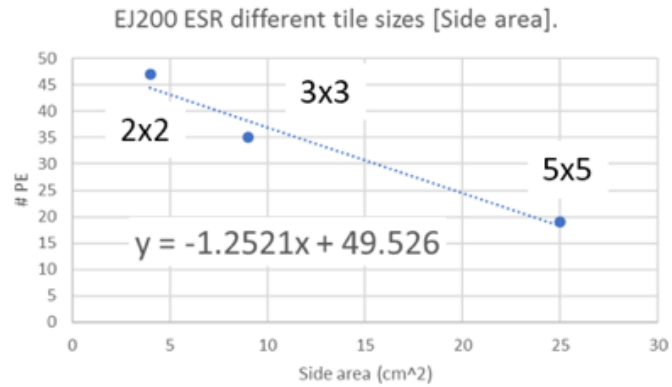


Figure 9: Light yield vs area of 3.8mm thick SIPM-on-tiles.

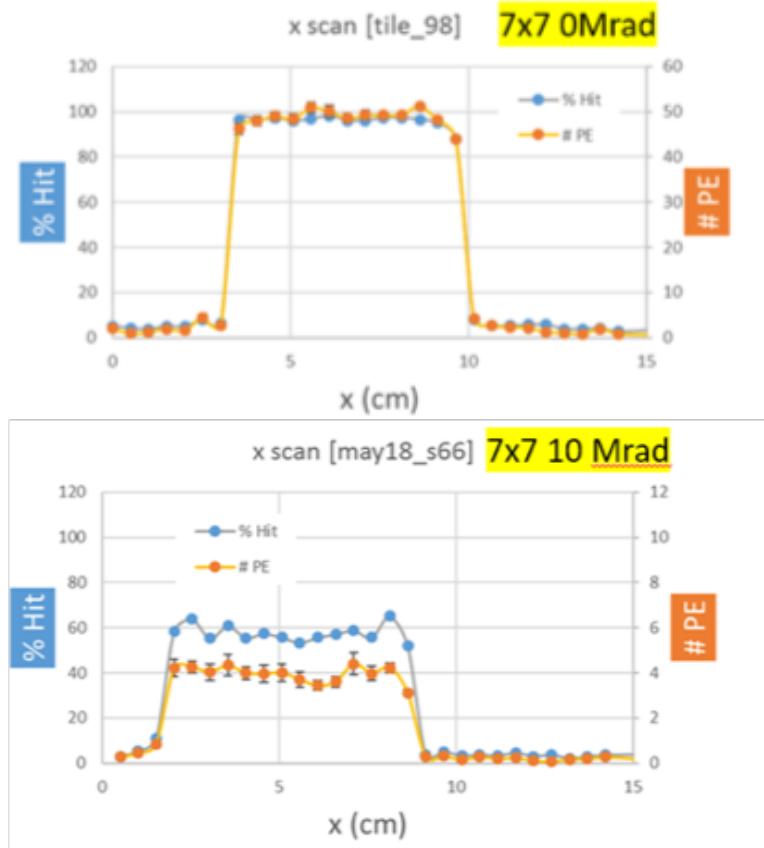


Figure 10: Light yield (LY) vs position (photoelectron uniformity scan in blue) for 7x7 tile with WLS fiber imbedded in it. Top: 0 Mrad. Bottom: 10 Mrad. We see that the tile LY remains uniform in x, even though the radiation damaged tile LY has dropped by almost a factor of 10.

## 7 T1044: sPHENIX Calorimeter Test

*R. Belmont, S.Boose, M.Conners, J. Haggerty, K. Hill, A. Hodges, J. Huang, E. Kistenev, J. Lajoie, E. Mannel, J. Osborn, C. Pontieri, M. Purschke, M. Sarsour, A. Sen, M. Skoby, S. Stoll, F. Toldo, B. Ujvari, C. Woody*

**Beam used:** Mixed Mode Pions/Primary Proton

**Run dates:** February 21 to March 27, 2018, April 27 to May 5, 2018 and May 17- 20, 2018

### Motivation and Goals

The goal of the 2018 T-1044 running was to test the high rapidity sections of the sPHENIX electromagnetic and hadronic calorimeters along with production front end electronics and the new sPHENIX digitizer system and compare the energy response to Monte Carlo simulations.

### Setup

The EMCal is a 2-D projective SpaCal design with scintillating fibers embedded in a tungsten powder infused epoxy. The HCal is a tilted steel plate with scintillating tiles design. Readout of both calorimeters uses a common set of electronics based on SiPMs as the optical sensors and having the amplified and shaped analog waveforms digitized with a 60 MHz sampling frequency. Initial testing of the EMCal was done with the EMCal located on the MT6.2C motion table to allow for a detailed scan of the detector. A combined test of the detector system was done on a table in the MT6.2D section of the FTBF beam line as shown in Figure 11. The detectors were oriented to simulate charged particles the striking the front of the high rapidity sections of the sPHENIX calorimeter system.

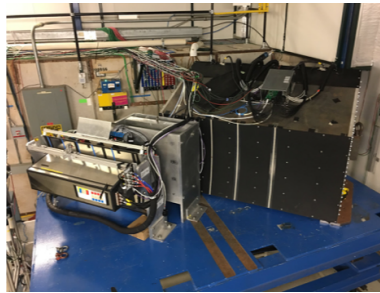


Figure 11: T-1044 setup in MT6.2D location. EMCal is on the left, inner HCal in the center and outer HCal on the right.



The detectors were readout using the production front end sPHENIX calorimeter electronics and waveform digitizer system operating with a 60 MHz sampling frequency. The resulting data along with trigger information, and data from Cerenkov system was recorded using the sPHENIX Data Acquisition system. Data was collected using pion beams from 1 to 60 GeV, both polarities and 120 GeV primary protons.

## Results and Publications

Analysis of the data collected during the 2018 running is ongoing to determine the energy resolution of the EMCal and HCal Calorimeters both independently and as a combined system. Figure 12 shows the preliminary energy resolution for a single tower in EMCal before and after a position correction is applied. The corrected energy resolution meets the requirements for the sPHENIX EMCal . Work is ongoing to complete the full analysis of the EMCal and HCal data and measure the combined system performance. Results of the data analysis for the EMCal, HCal, and combined systems are expected to be published in late 2018.

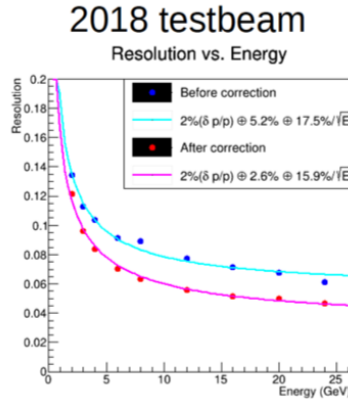


Figure 12: Preliminary energy resolution of a single tower in the EMCal before (blue curve) and after (red curve) a position dependent energy correction is applied.

## 8 T1068: Beam Test of the SVX4 Telescope

*Koji Nakamura, Shun Ono, Miho Yamada, Toru Tsuboyama, Kazuhiko Hara, Manabu Togawa, Minoru Hirose*

**Beam used:** 120 GeV primary protons

**Run Dates:** February 2018

### Motivation and Goals

The following three devices were tested at the beam test in FY18. 1) A planar type fine pixel detector which will be installed to the layer 2-4 of the ATLAS Inner Tracker (ITk) upgrade. 2) New fine timing resolution detector using avalanche gain technology (LGAD) for future general tracking detector which need timing resolution. 3) A monolithic SOI CMOS detector for future collider experiment as tentative target of ILC inner tracker. All three in development in Japan need precise measurement of the position resolution, detection timing, and precise position dependence on efficiency. To achieve this measurement high energy hadron beam is necessary and FTBF facility with 120 GeV proton beam is well suited to the requirements.

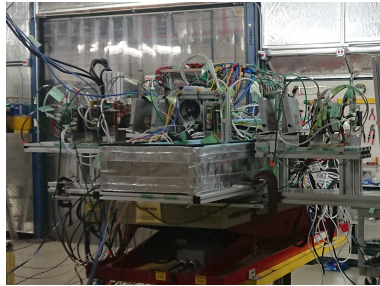


Figure 13: Setup of the ATLAS and LGAD detectors

### Setup

Two different set of position measurement detector (Telescope) and Detector Under Test (DUT) are located in MT6.2A and B area.

#### ATLAS and LGAD setup at MT6.2B

The Telescope is constructed by six layers of ATLAS pixel detector with FE-I4 ASIC ( $25\ \mu\text{m} \times 500\ \mu\text{m}$  pixel size) and 4 layers of SVX4 strip detector ( $50\ \mu\text{m}$  strip pitch). To

obtain better resolution, the device with odd layer number have been rotated by 90 degree. As DUT, LGAD detectors are placed at the middle of telescope. A picture for this setup is shown in Figure 13.

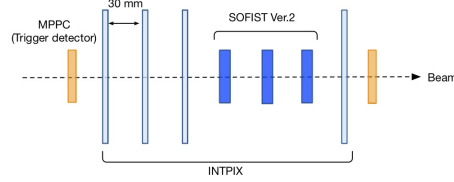


Figure 14: Setup of the SOI detectors.

## SOI setup at MT6.2A

The setup of SOI detectors consists of three SOFIST Ver.2 and four INTPIX chips (Figure 14). SOFIST Ver.2 is the prototype sensor for ILC vertex detector and has the pixel circuit for recording hit-timing and charge of incident particles. Each pixel has the comparator for signal discrimination and two memories to store up to two hits within  $25 \times 25 \mu\text{m}^2$ . INTPIX is the large area detector with the pixel pitch of  $17 \mu\text{m}$ . The INTPIX sensors were used as the telescope for the SOFIST.

## Results and Publications

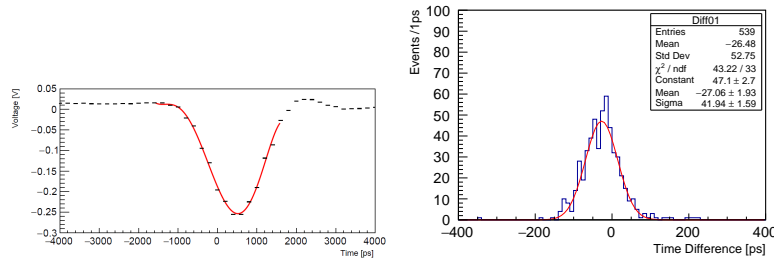


Figure 15: Typical signal shape of LGAD device (top) and measured time difference between two modules

## ATLAS and LGAD results

For the telescope operation successfully done and resulting less than  $10 \mu\text{m}$  pointing resolution obtained using rough alignment. New ATLAS pixel modules with RD53A chips

were also tested. Although no mature data taking system was available at that time, this experience was quite important to the following testbeam at CERN in July. The analog out signal of LGAD device are recoded using 5 G/s sampling flash ADC module and measured time resolution. Figure 15 shows typical signal gained by discrete amplifier (top) and timing resolution which is calculated using time difference between two LGAD device (bottom). As a result, time resolution for the single LGAD device is 29.7 ps.

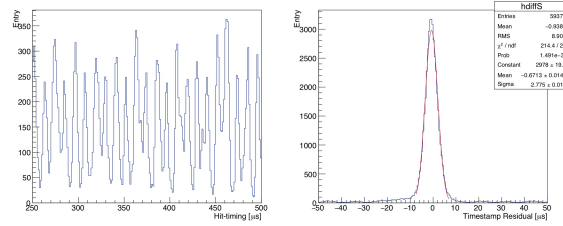


Figure 16: Hit-timing distribution (left panel) and difference between two SOFIST Ver.2 (right panel).

## SOI results

Distribution of the hit timings detected by SOFIST is shown in Figure 16. Thanks to fine time resolution of SOFIST ver.2, we can observe the bunch structure every 11 micro-second of FTBF beam. Figure 16 also shows the distribution of the hit-timing differences between two SOFIST sensors. The standard deviation became about 2.78 micro-second. The intrinsic time resolution of SOFIST Ver.2 was extracted about 2 micro-second.

K. Nakamura *et al.*, *Development of a radiation tolerant fine pitch planar pixel detector by HPK/KEK, Nuclear Inst. and Methods in Physics Research, A Accepted in 2018*, DOI:10.1016/j.nima.2018.09.015.

S. Ono *et al.*, *Development of a monolithic pixel sensor based on SOI technology for the ILC vertex detector, Nuclear Inst. and Methods in Physics Research, A Accepted in 2018*, DOI:10.1016/j.nima.2018.06.075

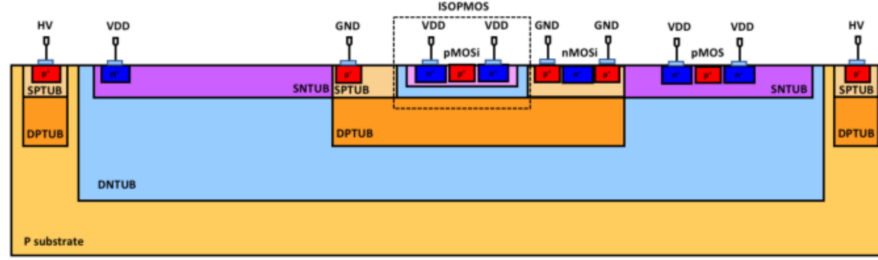


Figure 17: Left: The test beam setup includes 6 planes of pixel detectors and a cold box for the DUT. Right: The ATLASPix1 module.

## 9 T1224: ATLAS Pixel

*Jessica Metcalfe, Mathieu Benoit, Mateus Barreto Pinto Vicent, Vallary Bhopatkar, Wasikul Islam, Moritz Kiehn, Joseph Lambert, Joe Muse, Junjie Xie*

**Beam used:** 120 GeV Primary Proton

**Run dates:** Various

### Motivation and Goals

There were several objectives of the test beam period this year. The first was the installation of a new pixel telescope in section 1B that will remain as a permanent setup. This telescope is compatible with ATLAS pixel data acquisition systems and will be used for R&D by the Argonne pixel group as well as our international colleagues.

Several types of pixel sensors were tested. The first devices under test (DUTs) for this experiment were high voltage CMOS sensors, a candidate technology for the ATLAS Phase-II ITK Pixel Upgrade and a top candidate for future experiments. A standard CMOS process is modified to provide a deep n-well with high resistivity that can be biased to form an active region sensitive to charged particles. The ATLASPix1 CMOS sensor is a fully monolithic pixel module as shown in Figure 17. It requires an independent DAQ system and was thoroughly evaluated for the first time at the Fermilab Test Beam Facility.

The baseline pixel module for the ATLAS Phase-II ITK Pixel Upgrade uses a newly designed front-end read-out chip. The first prototype version, the RD53A, was fabricated in late 2017 and the first modules available in the spring. These modules were used to develop the DAQ system in order to integrate with the telescope.

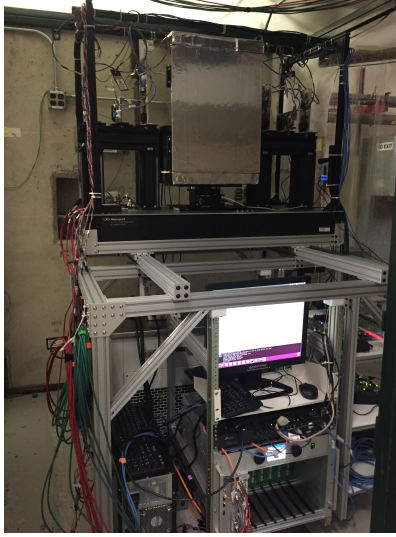


Figure 18: The test beam setup includes 6 planes of pixel detectors and a cold box for the DUT.

## Setup

The CMOS test beam was conducted between January 22nd and April 25th. Typically we used a 120 GeV proton beam with the maximum number of particles reaching around 3 million per spill. A pixel telescope was used to reconstruct tracks and then compare to the hits on the DUT. There were 6 planes of pixels with varying orientation to maximize the spatial resolution of the telescope. A cold box was available for the DUT that used air cooled by a chiller to reduce the temperature of the DUT. Details of this setup are shown in Figure 40. The telescope was installed in area 1B located in the MT6.1 'MTest' test area. The structural frame that the telescope sits on was built by the mechanical support team. The services of support personnel were invaluable to make small adjustments needed quickly in order to use the beam time most efficiently.

We also used the telescope from the University of Geneva in the 2B area for part of the CMOS testing.

## Results and Publications

The ATLASPix1 DAQ (Peary) was successfully integrated into the telescope setup and correlations were seen with the telescope and the CMOS DUT. Several unirradiated devices were tested and their performance evaluated. The track reconstruction efficiency is found to be greater than 99%. The results are shown in Figure 19. The test beam also enabled several areas of improvement for the design of the ATLASPix logic that will be implemented in

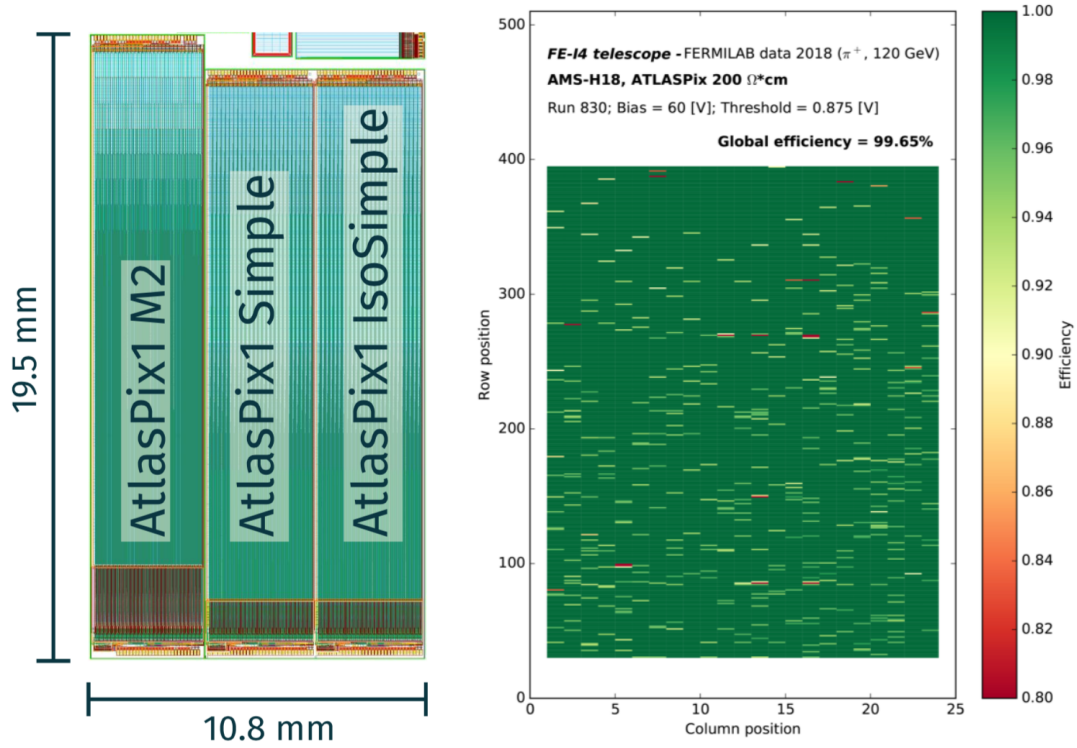


Figure 19: Left: The ATLASPix1 module layout. Right: Tracking efficiency map of the ATLASPix1 Simple matrix.

future versions. Results were presented in several ATLAS CMOS working group meetings, ITK Week, Upgrade Week meetings, as well as international conferences. In addition, the results from the FTBF were critical in the recent review of CMOS technology for use in ATLAS ITK Pixels.

The readout system for the RD53A module called Yet Another Rapid Readout (YARR) was integrated in to pixel telescope and a beam spot was observed as shown in Figure 20. This was achieved just before the summer shutdown and we plan to continue testing in the Fall.

#### Publications and presentations:

- *Performance of CMOS pixel sensor prototypes in ams H35 and aH18 technology for the ATLAS ITk upgrade*, Kiehn, Moritz, et al., NIM A, July 2018. <https://arxiv.org/abs/1807.05953>
- *Test beam measurement of ams H35 HV-CMOS capacitively coupled pixel sensor prototypes with high-resistivity substrate*, Benoit, Mathieu, et al., submitted to JINST December 2017. <https://arxiv.org/abs/1712.08338>

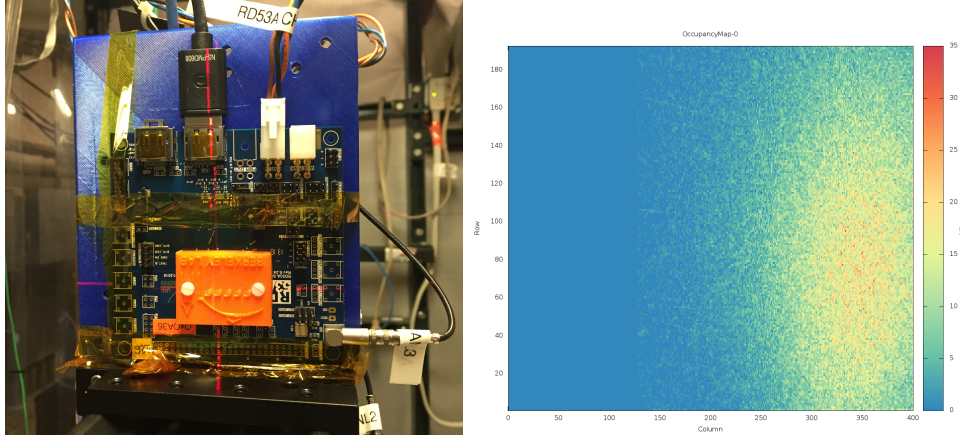


Figure 20: Left: An RD53A module installed in the FTBF. Right: Beam spot observed with an RD53A module.

## 10 T1396: EMPHATIC

*J. Paley, for the EMPHATIC Collaboration*

**Beam used:** 2 GeV to 120 GeV.

**Run dates:** January 2018

### Motivation and Goals

Hadron production uncertainties are a limiting systematic on accelerator and atmospheric neutrino flux predictions. The Experiment to Measure the Production of Hadrons At a Testbeam in Chicagoland, EMPHATIC, is a table-top-sized experiment designed to measure pion, proton, and kaon production cross sections on a variety of nuclear targets at beam momenta between 2 and 120 GeV/c, provided by the Fermilab Test Beam Facility. The dominant hadron production uncertainties are from interactions at beam energies below 20 GeV, which are inaccessible to current hadron production experiments. The main goals of the experiment are to measure the total cross section and double-differential cross sections involving pions, protons, and kaons in the final state across a broad range of momenta and nuclear targets, all relevant to accelerator and atmospheric neutrino fluxes. These measurements can reduce the current  $\sim 10\%$  neutrino flux uncertainties by a factor of two.



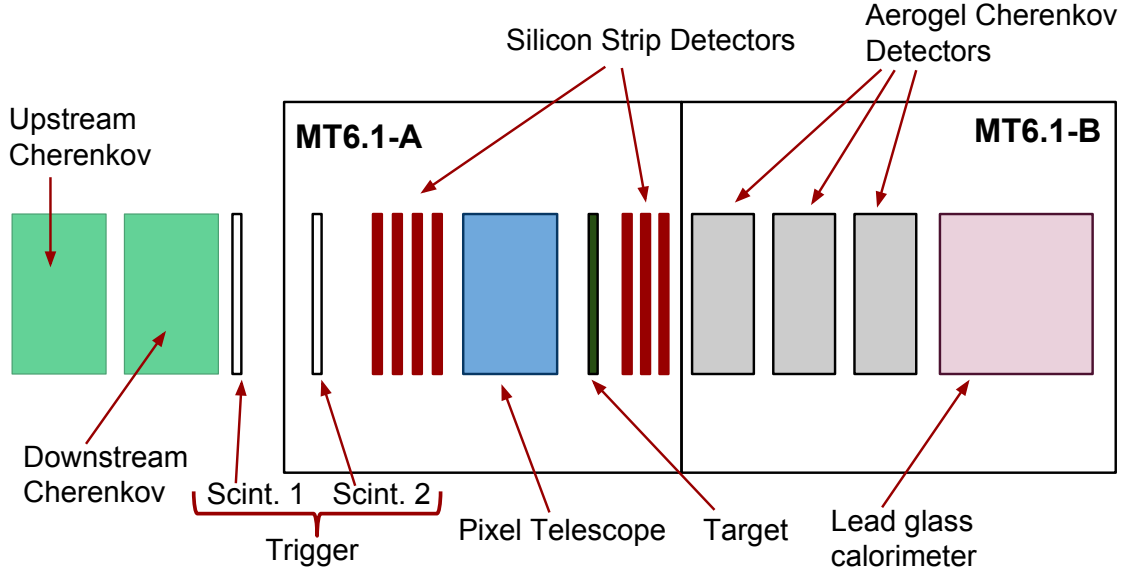


Figure 21: Schematic of the experiment setup during the January 2018 two-week run.

## Setup

The measurement of the total cross section requires excellent angular resolution. EM-PHATIC proposes to use emulsion films and silicon strip detectors for these measurements. The January 2018 run was aimed at gaining experience with these detectors, as well as understanding the performance of the beam. The experiment was set up in MT6.1a and MT6.1b, as shown in Fig. 21. All components except for the targets and aerogel Cherenkov detectors were provided by the FTBF.

The aerogel detectors were delivered by Chiba University (Japan) and TRIUMF Laboratory, although the highly transmissive aerogel itself all originated from Chiba University. Three different aerogels were used, one with  $n = 1.013$ , another with  $n = 1.026$  and another with  $n = 1.045$ . The aerogel blocks were installed in a light-tight mounting frame, and a PMT mounted to the frame. ADCs from each PMT were recorded in each event. The indices of refraction were chosen to enable beam particle identification for momenta between 2-8 GeV/c.

Data were collected with two different types of targets: emulsion bricks and bare thin targets. The emulsion bricks were a 5% interaction length piece of graphite, surrounded by three layers of alternating nuclear emulsion film, a thin acrylic plate and rohacell spacer material. The emulsion bricks were vacuum sealed in an emulsion handling facility at Lab 6, where the films were also developed after beam exposure. The dimensions of the emulsion bricks were approximately 10 cm wide, 5 cm deep and 5 cm tall. A motion table

was constructed for the experiment by TRIUMF collaborators that moved the emulsion brick a few mm in between spills. The position was recorded for every spill, and the beam trajectories reconstructed from the time-stamped silicon strip detectors will be matched to the beam trajectories reconstructed from energy depositions in emulsion films. A total of twelve emulsion bricks were exposed to approximately  $3 \times 10^5$  beam particles each, with the beam distributed across the face of brick. Two bricks were exposed to 120 GeV/c protons, and ten bricks were exposed 30 GeV/c beam. The energy depositions from all films have scanned and digitized at Nagoya University, and the internal alignment procedure for the films in each brick is underway.

The bare thin targets were 1-2 cm thick pieces of graphite, aluminum and steel, as well as empty-target for background subtraction. Approximately  $20 \times 10^6$  minimum bias triggers were collected using beam momenta from 2-120 GeV/c. Table 3 summarizes the number of triggers recorded at each beam momentum and target setting.

Momentum (GeV)	Graphite	Aluminum	Iron	Empty
120	1.63M	0	0	1.21M
30	3.42M	0.98M	1.01M	2.56M
-30	0.31M	0.31M	0.13M	0.31M
20	1.76M	1.76M	1.72M	1.61M
10	1.18M	1.11M	0.97M	1.17M
2	0.11M	0.11M	0.18M	0.11M

Table 3: Number of minimum bias triggers recorded on the different targets at the different beam momenta during the 2018 FTBF run.

## Results and Publications

Preliminary analysis of the data from the aerogel detectors indicates that very little light from the aerogel was recorded by the PMTs. The Chiba group has improved its aerogel production, and will be adding more and larger PMTs to these detectors in the future to address this issue.

As mentioned above, the emulsion data are currently being analyzed and calibrated. Although data from the pixel telescope were recorded, analysis of those data show the efficiency of the detector to be too poor to use. However, the analysis of the silicon strip detectors indicate efficiencies above 95%, and those data are being used to extract the total cross section by measuring the  $t \simeq p^2 \theta^2$  distribution, as shown in Fig. 22. In this plot,  $p$  is the beam momentum (30 GeV/c) and  $\theta$  is the angle between the reconstructed beam particle trajectory upstream of the bare thin graphite target and the trajectory downstream

of the target, using the data from the Si strip detectors. The collaboration is very focused on analyzing these data, and hope to publish results by the end of 2018.

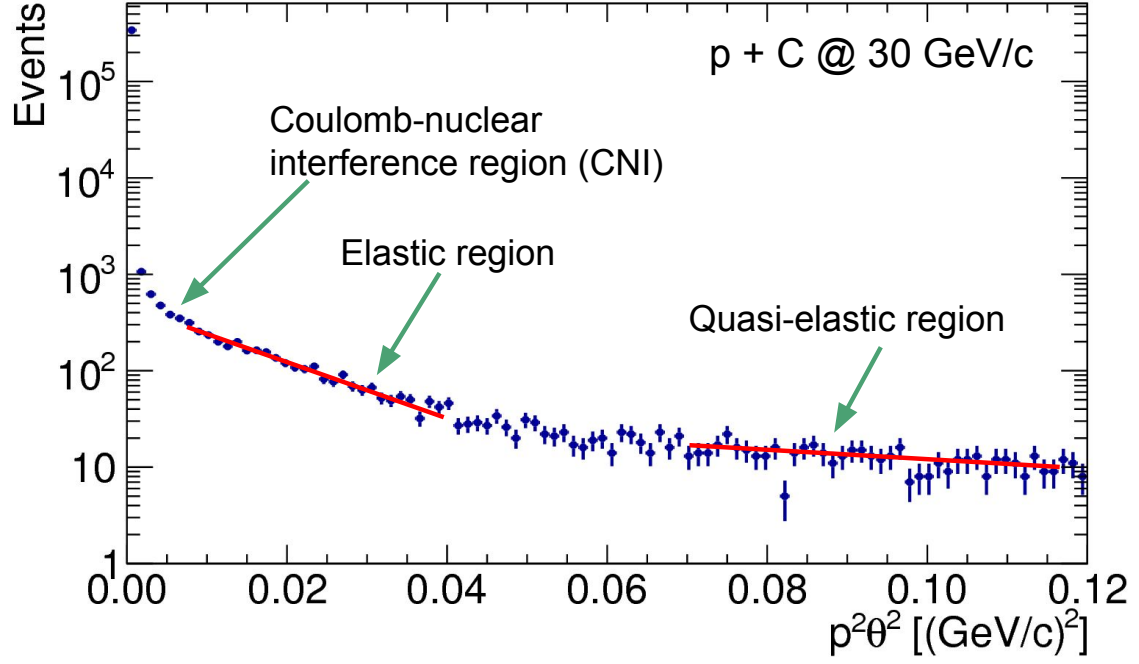


Figure 22: Outgoing  $t$  distribution of 30 GeV/c protons impinging on a graphite target.

## 11 T1409: CMS Timing Studies

*A. Apresyan, S. Xie*

**Beam Used:** 120 GeV protons

**Run Dates:**

### Motivation and Goals

During test beams at the FTBF in 2018 we studied several new prototypes of timing detectors for the CMS Phase 2 upgrades. The goals of these measurements were to establish a radiation hard technology capable to measure time of arrival of minimum ionizing particles (MIP) with a precision of 30-40 ps. The target application of these detectors is in High Luminosity LHC (HL-LHC) upgrades of the CMS and ATLAS detectors. At the HL-LHC an average of 140-200 pileup events will occur within a root mean square spread of approximately 5 cm along the beam axis, with a spread of 180-200 psec. The spatial overlap of tracks and energy deposits from these collisions will degrade the event reconstruction, and increase the rate of false triggers. Precision time stamping of all particles will add a new handle in discriminating the hard scatter from pileup interactions. If one imagines slicing the beam spot in consecutive time exposures of 30 psec, at HL-LHC the number of vertices per exposure drops down by a factor of 4-5, reducing the wrong associations to a level comparable to those observed without timing at the LHC. These enhancements translate into 20-40% increase in Higgs boson signal yield (depending on its decay channel), which directly translate into an increase in the effective luminosity.

### Setup

The Devices Under Test (DUTs) were mounted on a remotely operated motorized stage, placed inside the pixel telescope detector in FTBF Section 6.1A. The telescope provides better than 10  $\mu\text{m}$  position resolution for charged particles impinging on the DUT. Additionally, a Photek 240 micro-channel plate (MCP-PMT) detector was placed furthest downstream, and provided a very precise reference timestamp. Its precision has been previously measured to be less than 7 ps. Photographs of the experimental area are shown in Fig. 23. The DAQ system for the DUTs and the Photek MCP-PMT is based on a CAEN V1742 digitizer board, which provides digitized waveforms sampled at 5 GS/s, and with one ADC count corresponding to 0.25 mV.



Figure 23: A picture of the experimental area. The pixel telescope detectors are placed inside the electrostatic-discharge shielded boxes on the two sides of the DUT area. Cold box with mounting frames for LGAD sensors is shown on the right.

## Results and Publications

We had three very successful campaigns in FTBF during 2017-2018 season, and three more are planned in 2018-2019 season. Prototypes for CMS barrel and endcap detectors have been tested: SiPM+LYSO modules for the barrel region, and LGAD silicon sensors for the endcap. We have performed detailed characterizations of these technologies, and these studies helped to define the technology choice for the CMS upgrade program. Utilizing the unique telescope capability at FTBF, we measured with high precision the uniformity of sensor properties across their surface, and performed detailed characterizations of irradiated prototypes.

LGAD sensors produced by Hamamatsu, CNM and FBK were tested in past test beams. In order to cover the area of the detectors as large as CMS or ATLAS experiments, sensors should be manufactured in relatively large sizes, and have a large fill factor. In our measurements we demonstrated the high response uniformity of these sensors, as well as the gap size between pixels, as shown in Fig. 24.

Measurements of the time resolution and the response uniformity of the SiPM+LYSO modules of the barrel timing layer (BTL) detector prototypes are shown in Fig. 25. These measurements contributed significantly to the BTL sensor design and engineering.

These results have been published in NIM A 895 (158-172), and presented in the CMS Technical Proposal of the MIP timing detector. The data acquired during these test beams is now being used by an international team of physicists and engineers to design an Application Specific Integrated Circuit for the Phase 2 project.

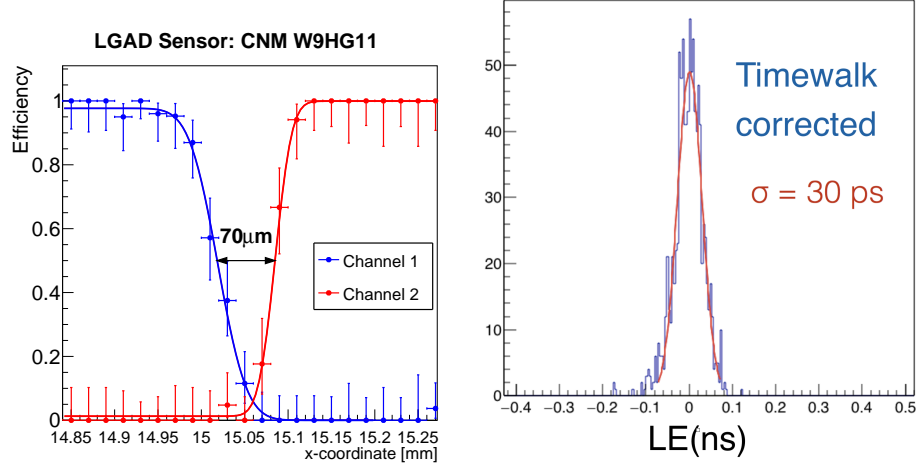


Figure 24: (Left) Efficiency measurement across the X-axis of the CNM 4-channel sensor. Data points in blue are those from one pixel, and those in red are from the neighboring pixel. Arrows indicate the distance between the half-maximum points of the fitted curves. (Right) Time resolution measurement of the FBK sensors with Carbon implant after  $8 \times 10^{14}$  n.eq/cm<sup>2</sup> fluence.

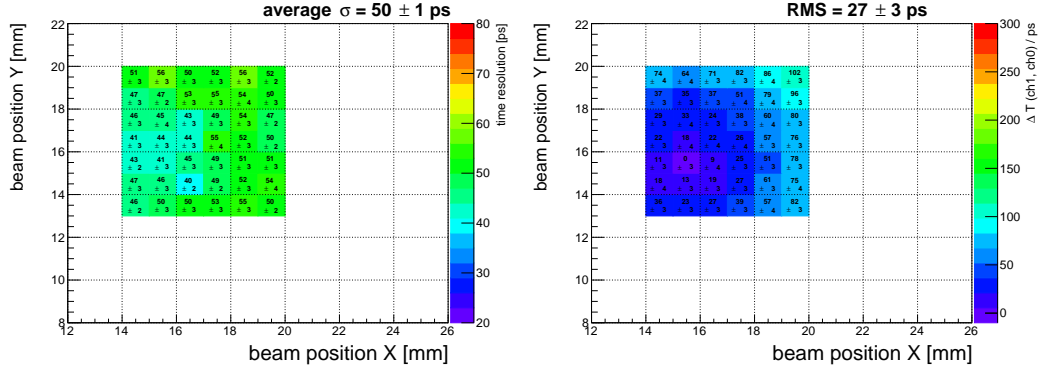


Figure 25: Measurement of the time resolution (left) and time offset (right) of the barrel timing layer prototype sensors, with SiPM coupled to a LYSO crystal, as a function of the MIP impact position of the LYSO surface.

## 12 T1429: Performance Study of a planar GEM and MM detector with zigzag pad readout

*S. Aune, B. Azmoun , A. Kiselev, I. Mandjavidze, H. Pereira-Da-Costa, M. Purschke, M. Vandenbroucke, C. Woody*

**Beam Used:** 120 GeV Protons

**Run Dates:** March 4-27, 2018

### Motivation and Goals

Our overall R&D goal is to optimize the geometry of zigzag shaped charge collecting electrodes for the readout plane of a variety of particle detector applications. The interleaving of the zigzag structure significantly enhances charge sharing between neighboring pads compared to more standard rectangular ones. Thus, a relatively large pitch can in principle offer high position resolution with a minimal number of instrumented channels, which greatly saves on cost and complexity. The objective of this beam test is to study the dependence of the detector performance on the physical parameters that define the zigzag pattern for various MPGD devices, including a planar GEM and micro-megas (MM) detector, in addition to a hybrid of the two.

### Setup

The apparatus under test includes a pair of quadruple GEM detectors and a pair of MM detectors equipped with similar readout planes consisting of an array of 100 1cm x 1cm cells, each with of a unique set of zigzag shaped pads. The detectors were mounted back to back, to a common XY-moveable stand which translates the detectors in a plane orthogonal to the beam axis and allows the beam to scan the full acceptance of each detector simultaneously.

### Results and Publications

By scanning an interesting range in the parameter space of the zigzag geometry, we are able to reveal fundamental behavioral trends and identify the most optimal parameter set for each detector technology.



Figure 26: Detector setup in beamline, including use of FTBF Si telescope.

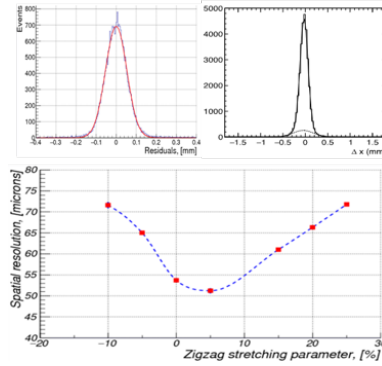


Figure 27: Top: Preliminary position resolution measurements for GEM and MM are between  $50\text{-}90\mu\text{m}$  Bottom: position resolution vs. zigzag stretching parameter.



## 13 T1439: sPHENIX Silicon Strip Tracker (INTT) Testsu

*Rachid Nouicer, Yasuyuki Akiba, Edmond Desmond, Masuda Hidekazu, Gaku Mitsuka, Itaru Nakagawa, Robert Pisani, Takashi Hachiya, Yorito Yamaguchi*

**Beam Used:** 120 GeV

**Run Dates:** March 2018

### Motivation and Goals

The study of the properties of hot and dense QCD matter, in particular, it's deconfined Quark-Gluon Plasma (QGP) state, is one of the main areas of nuclear physics research described in the US 2015 NSAC Long-Range Plan in which it is stated that "the upgraded RHIC facility provides unique capabilities that must be utilized to explore the properties and phases of quark and gluon matter in the high temperatures of the early universe and to explore the spin structure of the proton."

In this context, the sPHENIX collaboration at RHIC proposes a major upgrade to the PHENIX detector by constructing an entirely new spectrometer based on the former BaBar solenoid magnet. This upgrade, sPHENIX, enables an extremely rich jet and beauty quarkonia physics program addressing fundamental questions about the nature of the strongly coupled quark-gluon plasma, discovered at RHIC. The INTermediate Tracker (INTT) is a part of the particle tracking detectors of sPHENIX. The INTT detector consists of four barrel layers of silicon strip detectors (radius : 6, 8, 10, 12 cm) covering an acceptance of pseudorapidity within  $\pm 1.1$ , and a  $2\pi$  in azimuth.

A prototype of the INTT silicon telescope consists of three silicon strip half ladders was tested at the Fermi National Accelerator Laboratory (FNAL) Test Beam Facility as experiment T-1439 in March 2018. The INTT silicon telescope test setup and preliminary result obtained from the proton beam at 120 GeV are presented.

### INTT Silicon Telescope Beam Test Setup and Results

The INTT silicon telescope consists of three silicon strip half ladders mounted in a dark box, as shown in the Figure 28. Each half ladder consists of one flexible circuit boards called High Density Interconnect (HDI). Each HDI (approximately 493  $\mu\text{m}$  thick, 400 mm long, and 38 mm width) provides the slow control, power, and bias input lines as well as slow control and data output lines. The HDI carries two AC-coupled silicon strip sensors single side. Both silicon sensors, type-A and -B, have the same width 2.25 cm, pitch of 78  $\mu\text{m}$  in azimuth direction, and thickness 320  $\mu\text{m}$  but a different length 13.0 cm and 10.2 cm, respectively. The two silicon sensors are located in the middle of the HDI, and 13

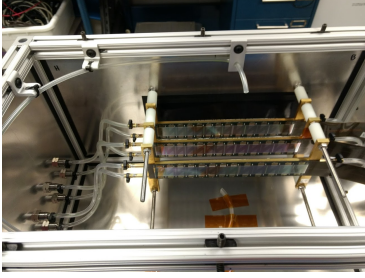


Figure 28: Picture of the INTT silicon strip telescope used at the test beam facility as experiment T-1439 in March 2018 (FNAL).

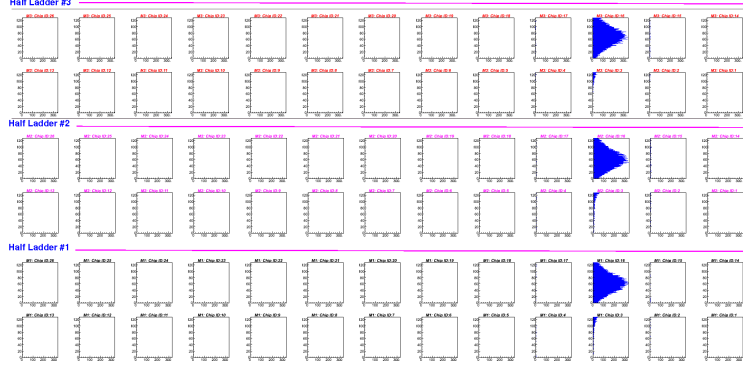


Figure 29: Measured hits distributions in the three silicon strip half ladders of the INTT telescope obtained during proton beam at 120 GeV. The x-axis and y-axis of the plot correspond to the number of hits and silicon strip number, respectively.

FPHX chips in each side of the sensors. The FPHX chip consists of 128-channel front-end ASIC, and was designed by Fermilab for the PHENIX/FVTX detector [1]. The chip was optimized for fast trigger capability; a trigger-less data push architecture, and low power consumption (64 mW/chip). Each half ladder is mounted on one support structure made of Carbon-Fiber-Carbon composite carrying two cooling aluminum tubes. Each half ladder is readout through an extender cable. The HDI end is connected to an extender cable which is connected at the other end to a Read Out Card (ROC). The extender cable is 40 cm long to reach the ROC. This is the first time we test the INTT silicon strip detector with the full readout chain in beam condition. Using this silicon telescope, we aim to study the detector response such as a signal-to-noise, and spatial tracking resolution using the proton test beam.

Figure 29 presents hit distribution measurements observed in the three silicon strip half ladders of the INTT telescope using proton beam at 120 GeV. The x-axis and y-axis of the plot correspond to the number of hits, and silicon strip number, respectively. Clearly, we observe a very good correlation, same chips' ID, of the hits' distributions in the three half ladders using proton test beam. We should also point out that silicon strips with no hits have a very small amount of noise. In conclusion, the INTT silicon telescope shows a very good performance with the proton beam at the Fermilab test beam facility.

**Acknowledgements:** We would like to thank the management and technicians of the Fermilab Test Beam Facility for their supports during our experiment T-1439 in March 2018.

**References**

- [1] J. Hoff, T. Zimmerman et al. , IEEE Nuclear Science Symposium Conference, 75 (2009).

## 14 T1441: sPHENIX MAPS Vertex Detector (MVTX)

*Hubert van Hecke, Sanghoon Lim, Ming Liu, Darren McGlinchey, Alex Tkatchev, Sho Uemura*

**Beam used:** Mixed Mode Pions/Primary Proton

**Run dates:** February 21 to March 27, 2018, April 27 to May 5, 2018 and May 17- 20, 2018

### Motivation and Goals

The MAPS Vertex Detector (MVTX) is a proposed upgrade to the sPHENIX experiment planned for the Relativistic Heavy Ion Collider (RHIC) at Brookhaven National Laboratory. MVTX will consist of three concentric layers of ALPIDE (ALice PIXel DETector) sensors, developed by the ALICE collaboration at CERN. Use of the latest Monolithic Active Pixel Sensor (MAPS) technology allows for a compact and thin design with low power consumption and a high degree of segmentation.

The goals for this test beam were to verify the tracking performance of the ALPIDE sensor in various occupancy environments, and prove the detector electronics and readout. MVTX will use the ALPIDE sensor and frontend FPGA board (“Readout Unit”) developed by ALICE, a backend FPGA board (“FELIX”) developed by ATLAS, and a DAQ system developed by sPHENIX; a test beam would demonstrate successful integration of these components in a working system.

### Setup

We set up at the downstream end of the MT6.2B area, downstream of the T1439 experiment (sPHENIX silicon strip tracker) and upstream of T1044 (sPHENIX calorimetry).

The system under test consisted of a telescope with four ALPIDE sensors, mounted on carrier PCBs inside a light-tight box (see Figure 30). We are grateful to the Fermilab SiDet facility for mounting and wirebonding two of the sensors on short notice. The Readout Unit was set up under the telescope box, and communicated over fiber to FELIX in the control room.

The DAQ was triggered on the FTBF scintillator coincidence (“SC1+SC2+SC3+Spill”). Most data was taken with a 120 GeV proton beam. Some runs were taken with lead bricks just upstream of the telescope, to create high-multiplicity shower events. For the last runs we mounted the telescope on a rotary table for tests of tracking at off-normal incidence.



Figure 30: (Left) The telescope box, with cover removed. Beam direction is from lower left to upper right. (Right) sPHENIX detectors in the MT6.2 area, beam is left to right.

## Results and Publications

The test beam operation successfully characterized the tracking performance of the ALICE ALPIDE sensor and determined that it meets the requirements of the sPHENIX MVTX detector. We observed excellent spatial resolution as shown in Fig. 31 (left) and cluster finding efficiency  $> 99.5\%$  as shown in Fig. 31 (right) for all 4 layers of the telescope, well above the MVTX requirements. This data is also important for validating the MVTX simulations used in the full sPHENIX tracking configuration, allowing for better understanding of the tracking capabilities and their impact on the physics performance of sPHENIX.

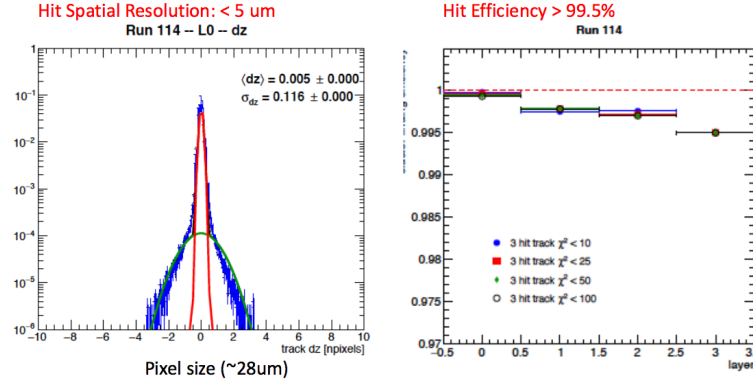


Figure 31: (Left) Displacement between track projection and cluster position in a single sensor. (Right) The cluster finding efficiency per layer for different 3-hit track quality cuts.

The successful operation of the full MVTX readout chain in the test beam was a key proof of concept for the MVTX review held at Brookhaven in July 2018. The review committee was impressed with the progress of the readout systems integration and recommended that MVTX proceed with procurement of the Readout Units.

## 15 T1443: SBND Vertical Slice Test

**Beam used:** LArIAT Tertiary Beam

**Run dates:** June 2018

### Motivation and Goals

Using the LArIAT detector we setup a Vertical Slice Test to test the electronics from SBND. The goals for the test were: Test the TPC readout electronic systems, exercise the DAQ, test slow control, test online monitoring, and find out the noise level for the SBND electronics.

### Setup

The left photo in Figure 32 shows the LArIAT TPC. The SBND electronics is shown on the top of TPC and a shield copper plane to protect the electronics from the High Voltage was installed. The right photo in Figure 32 shows one of the board from the SBND we tested. Figure 33 is the LArIAT setup with the SBND electronics .

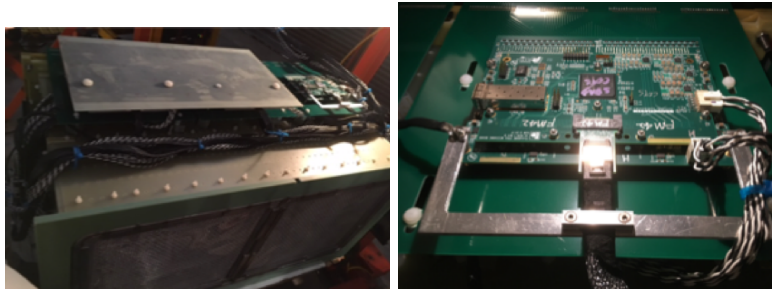


Figure 32: Left: LArIAT TPC with SBND electronics. Right: SBND board.

### Results and Publications

We have operated a complete vertical slice test of the readout system. Successful trigger readout stream, data acquisition, slow control and data quality monitoring. However, we encountered some issues with the high voltage (corrupted data and dead channels), possible discharges that damaged the boards. These issues are under investigation and a new cosmic run might be needed. Results are shown in Figure 34 and Figure 35.

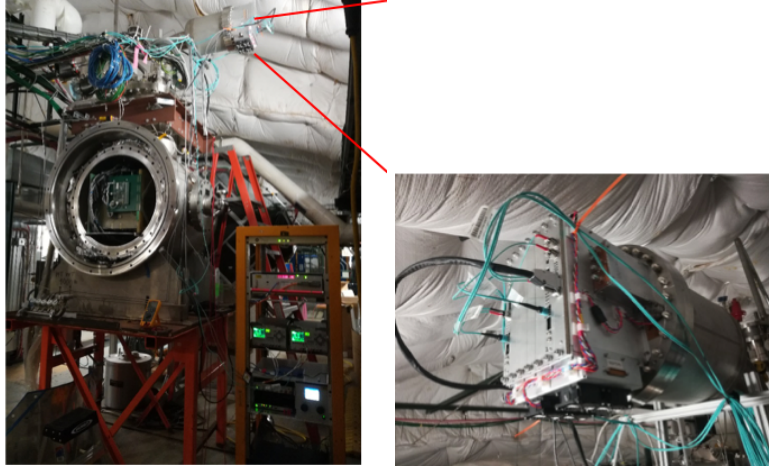


Figure 33: Full LArIAT Setup.

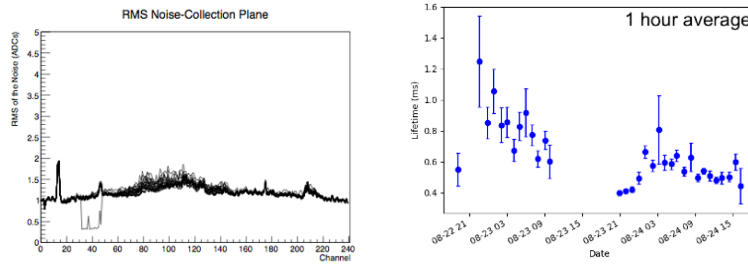


Figure 34: Left: Example of RMS of the noise vs channel number for different subruns. Right: Electron lifetime versus date.

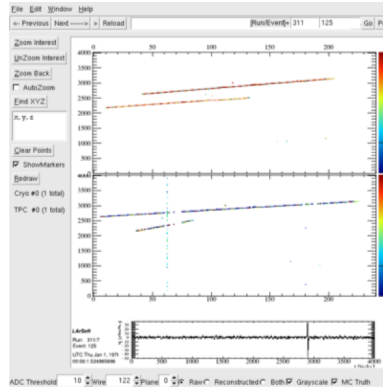


Figure 35: Example of cosmic muon tracks collected during run 2.



## 16 T1450: EIC PID R&D: Argonne MCP-PMT Test

**Beam used:** Mixed Mode Pions/Primary Proton

**Run dates:** February 21 to March 27, 2018, April 27 to May 5, 2018 and May 17- 20, 2018

### Motivation and Goals

As part of the eRD14 consortium developing PID detectors to be used at the EIC, we are developing pixelated LAPPD-style micro-channel plate PMTs (MCP-PMTs). Pixelated MCP-PMTs are required for imaging detectors such as RICH or DIRCs. We tested the rate capability and position resolution of copper pixel pads from 2x2 to 4x4 mm<sup>2</sup> in size.

### Setup

The ANL demountable is a stack of a Boro33 window with an Al photocathode, 2 Incom MCPs, and a pixelated PCB to form a MCP-PMT. The MCP-PMT stack is housed inside a vacuum chamber, as shown in Figure ?? . The PCB consisted of 4 sections of 2x2, 3x3, 4x4, and 5x5 mm<sup>2</sup> pads, with 16 channels arranged in a 4x4 square configuration in each section. The MCP-PMT was arranged in the beam-line with trigger scintillators in front and behind, and read out in coincidence with the FTBF MWPCs 1 and 2. Data were taken for the 2x2 to 4x4 mm<sup>2</sup> pads.

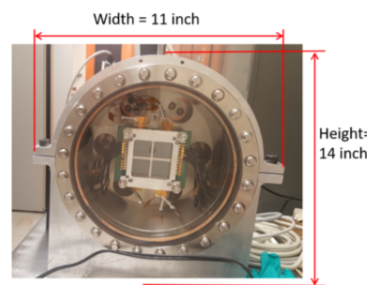


Figure 36: ANL Pixelated 6" MCP-PMT, Demountable

### Results and Publications

To determine the position resolution, we took the difference between the projection from the MWPC hits onto the MCP-PMT plane, and the position determined by the MCP-PMT pixel hits. Since the MCP-PMT electron cloud is rather small (less than 1mm), there was



little charge sharing between pads. In such cases the position was taken as the center of the pad. The difference between the MWPC and MCP-PMT determined positions is shown in Figure 37 for the  $2 \times 2 \text{ mm}^2$  pads, resulting in a sigma of 0.73 mm, consistent with expectations. The resolutions for the  $3 \times 3$  and  $4 \times 4 \text{ mm}^2$  pad runs were 0.94 and 1.4 mm, respectively. This was the first measurement of LAPPD-style MCP-PMTs with pixelated readout.

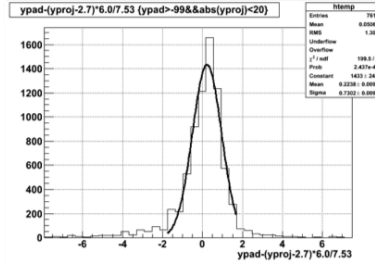


Figure 37: position as determined by the MWPCs, and the position determined by the MCP-PMT pixels.

## 17 T1450: EIC PID R&D: Argonne MCP-PMT Test

**Beam used:** Mixed Mode Pions/Primary Proton

**Run dates:** February 21 to March 27, 2018, April 27 to May 5, 2018 and May 17- 20, 2018

### Motivation and Goals

The experimenters are part of the eRD14 Collaboration developing detectors to be used at Electron-Ion Collider (EIC) experiments for particle identification (PID). One of the key PID detectors based on the ring imaging Cherenkov technology is a modular RICH (mRICH) developed by the collaboration for kaon and pion identification in momentum range from 3 to 10 GeV/c. This detector could also be used for pion and electron identification below 1.5 GeV/c. The first mRICH prototype was successfully tested at Fermilab in April of 2016 for demonstrating the working principles of this device and the test results have been published in NIM A. This test was to verify some of the PID performance with improved detector and readout electronics designs.

### Setup

The mRICH detector was set up on the movable table at MT6.2C as shown in Figure 1 (left panel). We also tried to take data with a set of two beam hodoscopes (not shown in the picture) but failed because of readout issues. We used extensively the signal and HV cables from FTBF and a portable chiller for stabilizing the temperature for testing a readout using silicon photomultiplier matrices. This test was run parasitically with SLYSUB experiments.

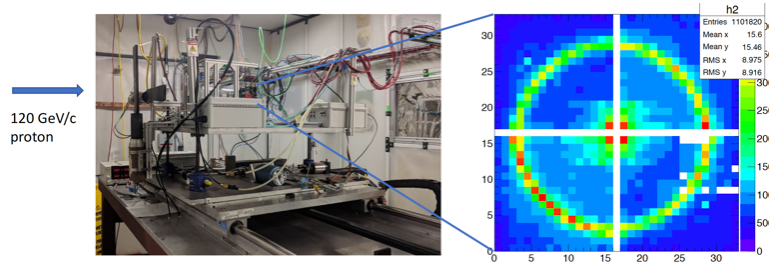


Figure 38: (Left) mRICH test setup in MT6.2C area; (Right) Cherenkov ring image detected on the photosensor plane of the mRICH.

## Results and Publications

This beam test was a great success. The picture on right shows a group photo after seeing the first online reconstructed ring image from mRICH. Some of the preliminary test results have been shown at the 10th RICH2018 conference very recently in Moscow.

The entire T-1048 team wants to express our sincere thanks for the unconditional support from the members of the FTBF at Fermilab led by Dr. Mandy Rominsky. We are looking forward to having the next round of test.

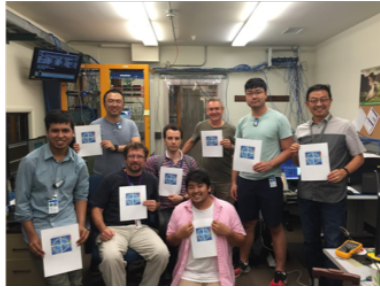


Figure 39: example caption

## 18 T1473: FLYSUB-Consortium Tracking and RICH Performance Evaluation

**Beam used:** Mixed Mode Pions/Primary Proton

**Run dates:** February 21 to March 27, 2018, April 27 to May 5, 2018 and May 17- 20, 2018

### Motivation and Goals

#### Large & Low Mass Triple-GEMs

The performance of two large and low-mass Triple-GEM detectors build at UVa and Florida Tech with different readout structures were studied at the test beam (T1037) in June - July 2018 at the FTBF. Florida Tech's prototype was constructed with carbon-fiber frames and has a 1D zigzag strip readout structure whereas UVa's prototype has a 2D U-V strip readout layer but was constructed with the more standard G10 frames. A small GEM prototype with a 2D zigzag strip readout structure (2DzzGEM) and a small  $\mu$ RWELL prototype where also tested in the beam test.

The main goal of the beam test was to study position resolution and basic detectors characteristics. The target of the ongoing GEM R&D is forward tracking at an EIC detector while the  $\mu$ RWELL technology can be view as a viable alternative for the TPC in for the central tracking region of an EIC detector.

#### seTPC

A Time Projection Chamber (TPC) prototype has been build for testing the space point resolution so it can be extrapolated in a future Electron-Ion Collider (EIC) experiment setup. We call this device seTPC to indicate its purpose within the sPHENIX/ePHENIX experiment.

### Setup

#### Large & Low Mass Triple-GEMs

The setup for the large and low-mass GEMs was located in the MT6.2b area of the FTBF as shown on Figure 40. The detectors under test consisting on the two large GEM prototypes, the small 2DzzGEM and the  $\mu$ RWELL prototype were all installed on the large MT6.2b moving table for position scan studies. A set of four small GEM Trackers provided by our colleagues from BNL were installed on two stations in front of and behind the moving table, in order to provide the tracking information needed for the position resolution studies. APV25-based Scalable Readout System (SRS) electronics was used to read out all detectors

(6.2k channels). Two SRS crates were set up near the large GEMs on the moving table. The detectors were operated with a 30Ar-70CO<sub>2</sub> gas mixture and occasionally Nitrogen (N<sub>2</sub>) for flushing. For the beam test, we were primarily interested in the 120 GeV primary proton beam, though we took data with 20 GeV hadron beam during one night shift to accommodate the request of colleagues running parasitically a beam test for mRICH R&D. Florida Tech's GEM prototype was initially mounted in the beam, but was subsequently removed from the beam as it was found that the detector could not hold full high voltage.

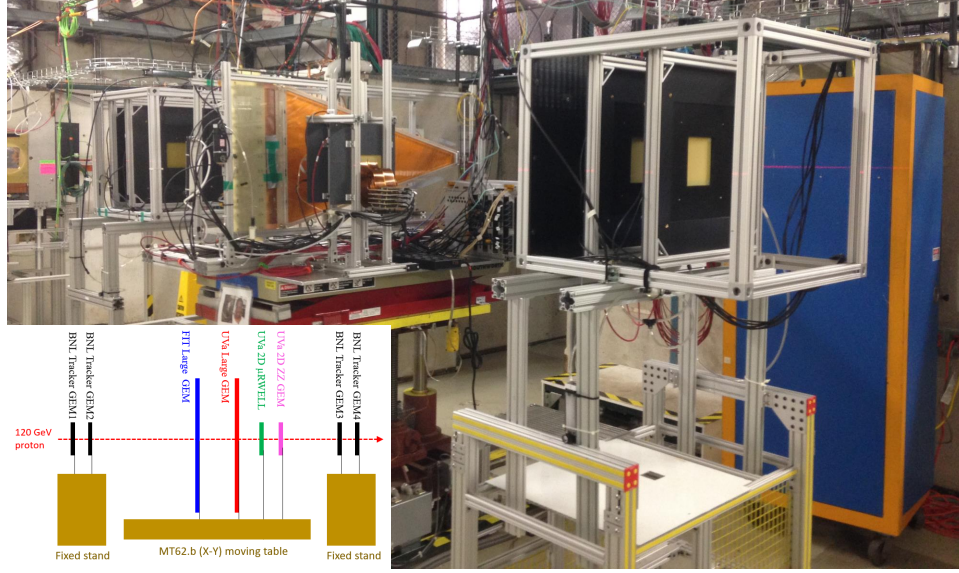


Figure 40: Large Triple-GEMs setup.

## seTPC

A TPC made out of a field-shaping foil, insulating polyimide foil and glass-fiber reinforced plastic layers that is similar in size as the inner field-cage of the seTPC was equipped with a quadruple Gas Electron Multiplier (GEM) amplification module and readout electronics (APV25). The TPC was placed on a  $8\text{ ft} \times 4\text{ ft}$  table (Fig. 41, left) and adjusted in height so that the beam would travel through the center of the volume. It was furthermore attached to a three-axis motorized stage which allowed to move along the TPC axis as well as to rotate around the roll- and yaw-axis. The TPC was operated with a Ne-CF<sub>4</sub> gas-mixture. The cathode side of the TPC was exposed to a high-voltage of about 20 kV and the whole setup was therefore secured by a shielded cage (Fig. 41, right).

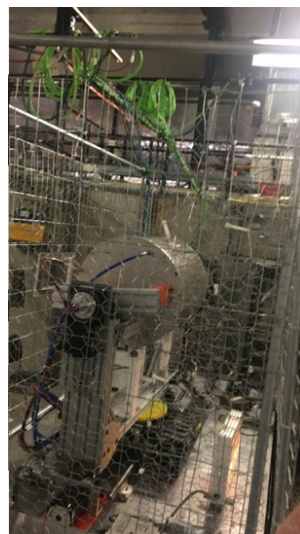
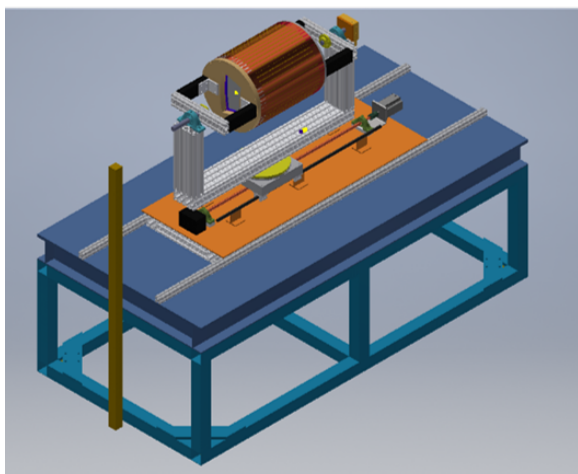


Figure 41: Left: Test-beam setup on a  $8ft \times 4ft$  table. Right: Photograph of the test-beam setup.

## Results and Publications

### Large & Low Mass Triple-GEMs

The analysis of the beam test data for the large low mass triple-GEM detectors is ongoing. Preliminary beam profiles of the 120 GeV proton beam and 20 GeV hadron beam on the U-strips and V-strips of the large UVa GEM prototype are shown on the top right plots of (Fig. 42). The top right and bottom left plots show the 2D reconstruction of the proton beam respectively with large UVa GEM and small  $\mu$ RWELL prototype. The four bottom right plots show the reconstructed 2D beam profile on the 4 BNL GEM trackers. The final goal of the analysis of the test beam data is to accurately extract the spatial resolution of the large Triple-GEM detector as well as for the small  $\mu$ RWELL and 2DzzGEM prototypes.

### seTPC

Analysis of the data has started and a preliminary set of tracks has been reconstructed (Fig. 43) as well as a preliminary beam profile (Fig. 44) established. The ultimate goal is to analyze the point resolution as a function of drift length with zero magnetic field from which one can obtain the resolution with magnetic field. This is an important result for making design choices of a TPC.

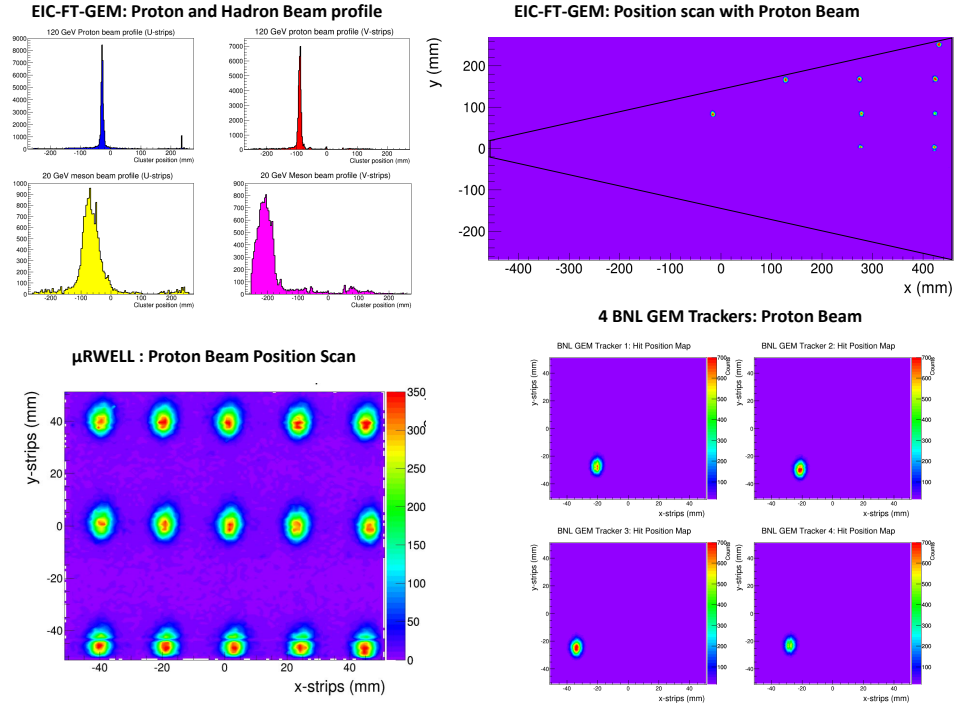


Figure 42: Beam profile on U and V strips of large UVa GEM (*top left*); 2D proton beam spot from position scan on the large UVa GEM (*top right*) and  $\mu$ RWELL detector (*Bottom left*); 2D Proton beam spot on the four BNL GEM trackers (*Bottom right*)

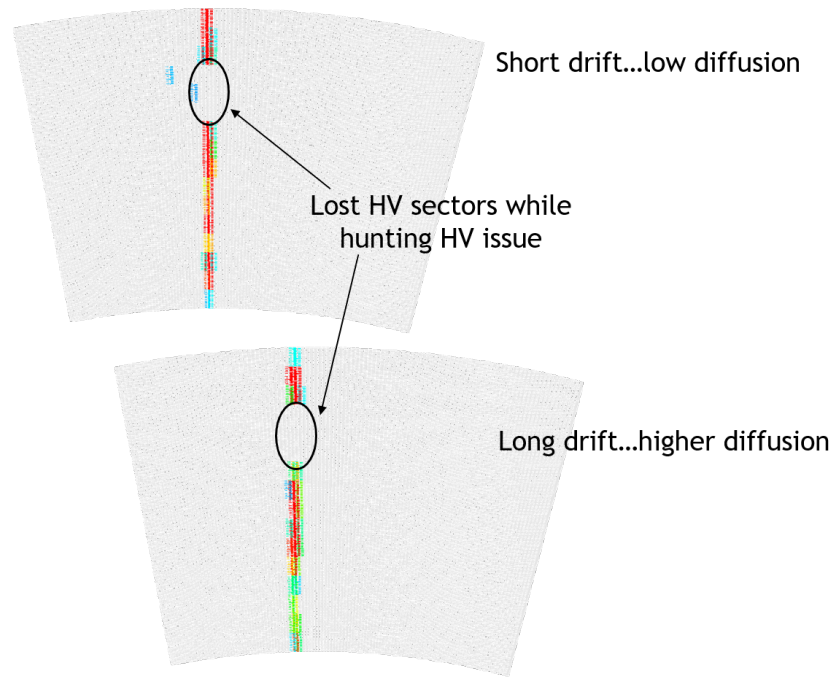


Figure 43: Two tracks at two different drift-lengths.

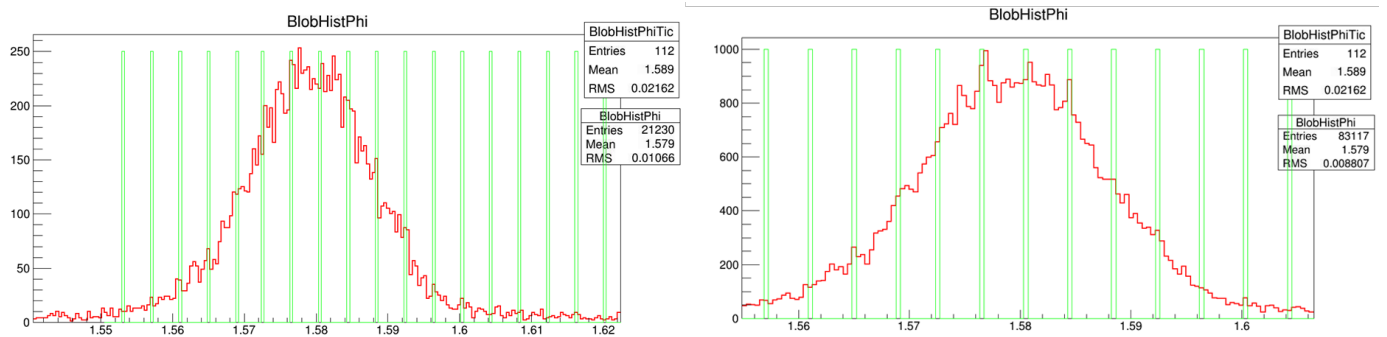


Figure 44: Beam profile as seen from two different pad rows. The green bars depict the centers of the pads.



## Personnel

Present at FTBF were two faculty, three research scientists, two post-docs, five graduate students, and four undergraduate students, one high school student.

## 19 T1473: sPHENIX TPC Prototype

**Beam used:** Mixed Mode Pions/Primary Proton

**Run dates:** February 21 to March 27, 2018, April 27 to May 5, 2018 and May 17- 20, 2018

*TK Hemmick, K Dehmelt, V Canoe-Roman, P Garg, N Ram, V Zakharov, L Legnosky, S Slote, I Yousuf*

**Beam used:** 120 GeV Primary Proton

**Run dates:** June 29, 2018 ? July 7, 2018

### Motivation and Goals

The sPHENIX experiment is an upgrade to the (now ended) PHENIX experiment at Brookhaven's Relativistic Heavy Ion Collider. The central tracking device for that experiment is planned to be a gate-less Time Projection Chamber (TPC) that will operate at both high rate and with high position resolution. Both of these goals are beyond the performance of current traditional TPCs. The goals are planned to be met using three basic design features:

- Micro-pattern gas detectors to reduce the Ion Back Flow (IBF) and thereby eliminate the complexity and deadtime from a standard gating grid.
- Very low diffusion gas to maintain precision over long drift distances (the full detector drifts for one meter and the prototype for 40 cm).
- Zigzag pad patterns with high incursion to ensure multi-pad hits even when the diffusion is very small.

This combination will allow sPHENIX to make the first measurement at RHIC that will be able to distinguish the three close-lying Upsilon states (1s, 2s, and 3s). In sPHENIX, the low diffusion ( $60 \mu\text{m}/\sqrt{\text{cm}}$ ) is assisted by the 1.4 Tesla magnetic field. At FTBF, we cannot apply this magnetic field and must thereby suffer higher diffusion more than triple the diffusion ( $200 \mu\text{m}/\sqrt{\text{cm}}$ ). We are nonetheless able to infer the eventual resolution of sPHENIX by using a clever analysis. The length dependence of position resolution in a TPC follows the expression shown below:

$$\sigma_{tot}^2(L) = \sigma_{int}^2 + D^2/N_{eff}L \quad (1)$$

Here  $\sigma_{int}$  is the intrinsic resolution of the pad plane, D is the diffusion constant, and  $N_{eff}$  is the number of effective electrons (reduced by some factor as compared to the total ionization due to effects such as gain fluctuations). The unknown factors that are

dependent upon detector design are  $\sigma_{int}$  and  $N_{eff}$ , both of which can be deduced from a simple fit of the resolution vs drift length as measured in beam. Following this, one can predict the performance of the TPC in sPHENIX by scaling the slope to account for the known small diffusion in magnetic field.

## Setup

The sPHENIX TPC is designed as a 1.6-meter diameter 2-meter long cylinder. High voltage is applied to the midpoint of the TPC ensuring limiting the electron drift path to 1 meter. The mechanical integrity is maintained at low radiation length using a honeycomb structure, and the field is shaped using a striped Cu-Kapton flexible circuit card.

The FTBF prototype TPC is built from identical materials and techniques as the main one, however the cylinder has only 40 cm diameter and 40 cm length. The prototype is a single ended TPC and thereby allows measurements of electron drift over the full 40 cm length, thereby giving enough lever arm that we can be expected to get good slope and intercept determinations from the length dependence of the resolution.

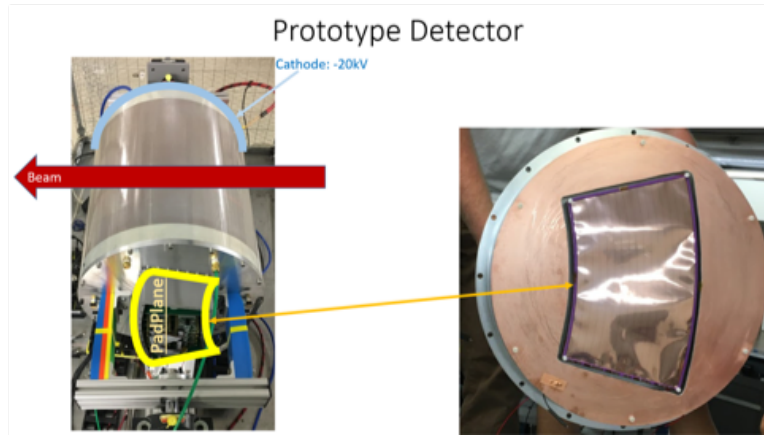


Figure 45: Detector in beam at FTBF.

## Results and Publications

The data analysis is proceeding very well. The final result shows an intrinsic resolution of our pad plane of  $70 \mu\text{m}$  and  $N_{eff} = 20.4$ . When combined with the known diffusion at high field, one gets an anticipated sPHENIX resolution for the full detector operating at full field as shown in Figure 46.

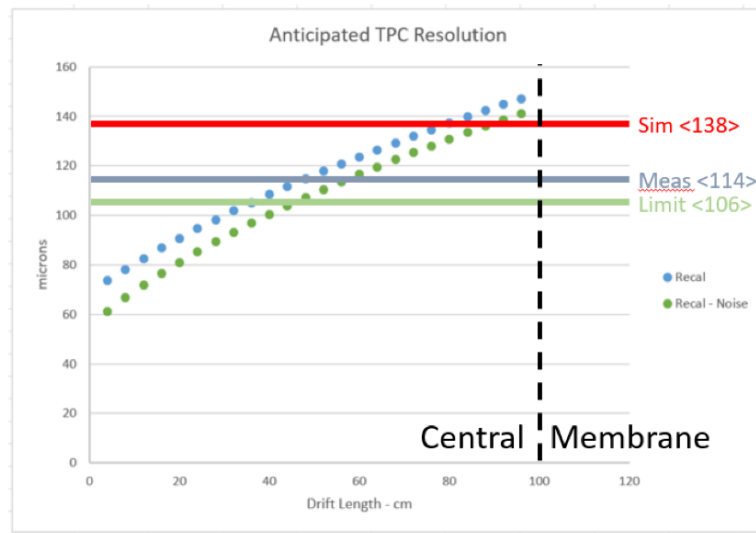


Figure 46: Anticipated field-on resolution for the full sPHENIX TPC based upon FTBF prototype measurements. This result is better than in the current sPHENIX simulations.

## A Publications

### T992: Tests of Radiation-hard Sensors for the HL-LHC

- *Pixel Detector Developments for Tracker Upgrades of the High Luminosity LHC*, M. Meschini (INFN, Florence) et al.. 2018. 7 pp., Published in Springer Proc.Phys. 213 (2018) 349-355
- *The Fermilab Test Beam Facility Data Acquisition System Based on otdaq*, Kurt Biery, Eric Flumerfelt, Adam Lyon, Ron Rechenmacher, Ryan Rivera, Mandy Romin-sky, Lorenzo Uplegger, Margaret Votava (Fermilab). Jun 19, 2018. 2 pp., FERMILAB-CONF-18-266-CD, (RT2018) Conference: C18-06-11.7
- *Beam Test Results of Thin n-in-p 3D and Planar Pixel Sensors for the High Lumi-nosity LHC Tracker Upgrade at CMS*, Irene Zoi (Hamburg U.) et al.. 2017. 6 pp., Published in PoS EPS-HEP2017 (2017) 809

### T1044: sPHENIX Calorimeter Test

- Paper has been submitted, waiting on final confirmation.

### T1068: Beam Tests of the SVX4 Telescope

- K. Nakamura *et al.*, *Development of a radiation tolerant fine pitch planar pixel de-tector by HPK/KEK,Nuclear Inst. and Methods in Physics Research*, A **Accepted in 2018**, DOI:10.1016/j.nima.2018.09.015.
- S. Ono *et al.*, *Development of a monolithic pixel sensor based on SOI technology for the ILC vertex detector*, *Nuclear Inst. and Methods in Physics Research*, A **Accepted in 2018**, DOI:10.1016/j.nima.2018.06.075

### T1224: ATLAS Telescope

- *Performance of CMOS pixel sensor prototypes in ams H35 and aH18 technology for the ATLAS ITk upgrade*, Kiehn, Moritz, et al., NIM A, July 2018.  
<https://arxiv.org/abs/1807.05953>
- *Test beam measurement of ams H35 HV-CMOS capacitively coupled pixel sensor pro-totypes with high-resistivity substrate*, Benoit, Mathieu, et al., submitted to JINST December 2017.  
<https://arxiv.org/abs/1712.08338>